KTH ROYAL INSTITUTE
OF TECHNOLOGY

KE200X Degree project in Chemical Engineering

Second Cycle, 30 credits

Carbon dioxide separation by disc stack centrifuge at low CO2 concentration

DAVID CORREA ZAPISOTSKI

Stockholm, Sweden 2022

ABSTRACT

As the world is going through a climate crisis, ways to mitigate it in the short and long term have been investigated. Carbon dioxide is a molecule of importance due to the amounts that are freely emitted into the atmosphere because of combustion processes. Due to this, one way of many, to mitigate climate change is Carbon capture and storage, CCS. There are also consequently several ways to capture and separate CO_2 in post combustion processes, such as the use of rotating packed beds or wetted wall columns, however the use of disc stack centrifuges has not been investigated for this application. This paper has investigated and used a disc stack centrifuge for this purpose, by using water and NaOH solution as aerosol absorbents. Some parameters have been varied such as NaOH concentration, air flow speed and carbon dioxide concentration. Results had shown that the use of a disc stack centrifuge did not yield considerable CO_2 separation, however, an explanation for this was found to be due to low CO_2 concentration and limited measuring instruments as well as a setup that did not make it possible for absorbent and CO_2 to fully react and be efficiently separated.

SAMMANFATTNING

Medan världen undergår en klimatkris, nya sätt för att mildra den har undersökts för den korta och långa loppet. Koldioxid är ett ämne som uppmärksammats då stora mängder av den släpps ut till atmosfären på grund av förbränningsprocesser. Med avseende om detta har ett sätt för att mildra klimatomställningen undersökts, ”Carbon Capture and Storage”, CCS. Det finns redan metoder för att fånga och separarera CO2, genom exempelvis roterande packade säng eller vattnade vägg kolumner. Dock har staplade disk centrifug inte undersökts. Denna rapport har undersökt och använt en staplad disc centrifug för just koldioxid separering, genom användning av vatten och NaOH-lösning som absorbenter. Några parametrar har varierats såsom concentrationen på NaOH-lösningen, luftflödeshastighet och koldioxid koncentration. Resultaten visade, att användning av en staplad disk centrifug, separarede märkvärdiga mängder av CO2. Det hittades däremot förklaringar till detta och det var att den låga halten CO2, de begränsade mätinstrumenten och det experimentella uppställningen som ej gav tid för absorption att ske.

FOREWORD

I would like to dedicate this foreword towards all of the people that helped me during the course of this Master Thesis Project, and as well by noting that this project has been a pleasure and insightful to be a part of for the past 8 months.

From 3Nine, the partner company for this project, I would like to begin by thanking Carl Häggmark, my supervisor, for helping me throughout the whole project and was willing to listen and help me at all times. Next, I would like to thank other employees of 3Nine that helped during some steps in the project, Peter Franzén, Dan Karlsson and Claes Inge.

From KTH, I would like to thank my examinator Christophe Duwig for all feedback and help I have received.

TABLE OF CONTENTS

1 INTRODUCTION

A growing and alarming concern for the future is the issue of climate change, and therein the causes of it. One of the causes of note is the emission of greenhouse gases, such as carbon dioxide, methane, nitrous oxide. These gases have been a contributing factor to the ongoing and upcoming changes in climate around the world. In particular Carbon Dioxide has been of main contention as it is emitted in large amounts compared to other gases, where combustion processes are a contributing factor to its emissions [6][24]. It has been warned for several years by the IPCC that if drastic cuts in emissions are not made by 2030, then the average temperature around the world will increase by over 1.5C°[25]. In the past few decades technology relating management of carbon dioxide has been developing called Carbon Dioxide Capture and Storage, *CCS*. In order to also maximize carbon capture, an optimal solution or solutions needs to be found.

In addition to growing concerns about emissions in a macro scale, there is also one of a smaller scale for the average work environment. In plenty of occupations there is a risk of being actively exposed to various harmful gases, Carbon Dioxide being one of them. This can by extension lead to health issues in time and cripple the worker's abilities, both physical and mental [9]. Such occupations range wide, examples include combustion related work, mining related work and transport related work. For transport related work there are big steps in order to shift the act of transporting from fossil to electric driven transport, both commercially and in industrial capacity. However, in work relating to mining and combustion, Carbon Dioxide is constantly emitted as a byproduct through various chemical processes. There are already legal limits on average Carbon Dioxide concentrations that one person can be exposed to in both long and short term. The Swedish Work Environment Authority has placed a limit on 5000 and 9000ppm for long- and short-term exposure respectively of Carbon Dioxide. However, elevated CO_2 concentrations also accompanies with an increased amount of other pollutants [35].

1.1 RELATION TO KTH SUSTAINABILITY GOALS

KTH is required, as every other higher level education institution in Sweden, to aid and promote sustainable development since 1992. Between then and today different ways of defining the goals have been made, one of which is the United Nations Sustainable Development Goals containing 17 categories of goals until 2030. These goals have been adopted by all members of the United Nations. KTH has also worked to integrate these goals into their action plans, in which education and research is included. This work relates heavily to goal 13, climate action, due to investigating into separation of Carbon dioxide, a heavily emitted greenhouse gas.

1.2 OBJECTIVE OF WORK

In this project, a centrifugal disc stack separator is used to separate aerosols which have absorbed Carbon dioxide. It is a separation technique that has not been studied in conjunction with Carbon Dioxide capture previously. Most research and use of this type of separator has

been applied towards separation of oil droplets. The goal is to conduct an experiment to test this method with two different absorbents and varying bulk flow rates, in conjunction with the use of a ultra-sonic transducer for aerosol generation.

2 LITERATURE SURVEY

In this chapter material related to the topic is reviewed and investigated. For CCS there are numerous methods applied and techniques applied. For this paper the methods that makes use of absorption in post combustion processes are looked at.

There are several technologies for CCS in use today, as well as in development. These are looked at in the next section. However, there is also a need to look at the absorbents used for these technologies.

Furthermore, a following process in which the absorbent is regenerated, and the reaction is reversed to separate Carbon Dioxide is also of note. The regeneration process is used in order to be able to recycle the absorbent without having to continuously input large amounts. This process is however out of the scope of the project and arre not be looked at in particular. The focus is mainly on Carbon Dioxide absorption and subsequent separation.

2.1 CARBON CAPTURE TECHNOLOGIES

In this section possible and current separation methods are briefed on, among them is the focus of the report, disc stack centrifuge.

2.1.1 DISC STACK CENTRIFUGE SEPARATOR

The disc stack centrifuge is a tool more commonly used to separate oil droplets from oil mist and within fermentation processes [4][12][32] To separate droplets, the centrifuge rotates at high speeds. The separator is shaped with various stacked discs that are diagonally oriented. The concept of the disc stack centrifuge hinges on separating particles that have a diameter larger than that of the critical. Particles of this size should theoretically be separated at efficiency of 100%.

In order to calculate the critical diameter, d_c, (Eq. 1) can be used, derived from Stoke's Law [1][10][27]:

$$d_c = \sqrt{\frac{18\mu Q}{A_e \Delta\rho g}} \qquad \text{(Eq. 1)}$$

This equation is validated for separation of solid particles by liquid, where $\Delta\rho$ is the density difference between liquid and solid. For liquid-liquid and liquid-gas separation the density difference is between both used liquids and liquid and the absorbed gas respectively; μ is the dynamic viscosity of the liquid; Q is the volumetric flow; A_e is the settling area of disc stack and g is the gravitational acceleration. Any particle above this critical diameter is said to be separated fully. However, in reality it is not possible to separate all particles, due to size constraints within the system. Particles below the critical diameter has been found to be separated at a probability given by (Eq. 2) [4][32] if Stoke's law is perfectly applied by the particles:

$$\eta(d) = \frac{d^2}{d_c^2}, if\ d < d_c$$

(Eq. 2)

For particles that do not perfectly follow Stoke's law this separation efficiency can be modified for particles of all sizes as seen in (Eq. 3) [4]:

$$\eta(d) = 1 - \exp\left[-\left(\frac{kd}{d_c}\right)\right]^n$$

(Eq. 3)

The newly introduced parameters, k and n, are derived from experimental methods.

2.1.2 WETTED WALL COLUMN

Wetted wall columns, WWC, have been studied for distillation and absorption purposes, both with similar mass transfer physics [19][38]. The setup usually consists of a tube, where a falling film of liquid is formed on the walls of the tube. The target gas flows in the opposite direction of the liquid. WWCs are not commonly used in wide scale applications and has been used more in lab scale experiments for research of mass transfer properties, it has limitations regarding total output which is not desirable for industrial applications separation technology. WWCs provides with high mass transfer rates.

2.1.3 ROTATING PACKED BED

A rotating packed bed, RPB, is commonly used for absorption, stripping and desorption processes. There also exists conventional packed beds, PB, however, RPB has been found to have a much higher mass transfer coefficient and higher flowrates of both liquid and gas has been found to be applied in comparison to conventional PBs. The packing of PBs in general, RBP included, consists of some form of mesh, several studies have used stainless steel wires [14][17][29]. The principle of RBP is that as the bed rotates the liquid and gas interact with each other from opposite directions.

2.2 CARBON CAPTURE ABSORBENTS

In this section various absorbents are discussed, both chemical and physical. However, first there needs to be clarifications in what the desirable absorbent properties are. To start with, the selectivity of the absorbent towards its target in relation to its surrounding environment is important to consider. A higher selectively would lead to a higher likelihood for the absorbent to react with the target.

Another property to consider is absorbing capacity of the absorbent. A lower capacity would mean that there would have to be a higher amount of the absorbent in the process compared to if the absorbing capacity would be high.

The reaction rate of the absorbent toward its target is also of note. A higher reaction rate would mean that the absorption is able to happen more swiftly during the capture process. The reaction mechanism is however differentiated between the physical and chemical processes. The physical absorption process is diffusion dominated and the chemical is reaction dominated.

Continuing, the toxicity of the absorbent and its reaction products is of importance to the health and safety of workers and the surrounding environment. And if a toxic absorbent is chosen, a solution to how it is handled should be brought forward regarding worker safety and disposal or handling of reaction products. Ideally a non-toxic absorbent should be prioritized. There is also the matter of the carbon footprint of the absorbent. If it is made through higher emissions of carbon dioxide or other acid gases in comparison to the carbon dioxide captured per unit of the absorbent, then the absorbent should not be used as it would defeat the purpose of carbon capture.

Furthermore, the cost of the absorbent ought to be considered, however, depending on the properties of the absorbent, the cost can be outweighed by them.

There are two types of absorbents, physical and chemical absorbents. Physical absorbents do not react with their target, and instead makes use of simple diffusion of the target into the absorbent through the liquid-gas interface, following Henry's law. The target in this case is Carbon Dioxide. Chemical absorbents on the other hand, react with their target and a chemical reaction is initiated between absorbent and target. From this a product is formed from the reaction.

The usage of these absorbents varies, physical absorbents are commonly used in natural gas sweetening processes, a process in which Carbon Dioxide is removed from the gas, to keep the natural gas pure and more effective at its applications [11]. Chemical absorbents are used for lower Carbon Dioxide concentrated gas streams, usually in post-combustion processes.

One bigger disadvantage of the use of chemical solvents is the regenerative step, which is not within the scope of this work, where it is an energy intensive process. Chemical solvents exist within a range of different classes of chemicals, ammonia based, hydroxide based, amine based, and carbonate based being the most researched types for the purpose of Carbon Dioxide capture.

Absorbents that are commonly used or have potential are briefed, they are also separated between physical and chemical categories as well as subcategories, for different types of chemical-based absorbents, in the following sections.

2.2.1 PHYSICAL ABSORBENTS

Selexol is a physical absorption process commonly used for Carbon Dioxide removal, it is also the trade name for dimethyl ethers of polyethylene glycol, thus Selexol is referred as the name of the solvent. Selexol is used in processes of temperatures above 300 Kelvin and pressures at around 30 atm [15][22]. It is ideally used in precombustion processes such as natural gas sweetening as mentioned earlier. Selexol has a disadvantage in pricing, as it is

relatively expensive compared to its chemical counterparts, this is partly due to high energy requirements for its production. On the other hand, Selexol has shown to be non-corrosive.

Rectisol is the trade name for cooled methanol used in absorption processes of Carbon Dioxide. The absorbent is used for lower temperature operations, below 0 degrees Celsius. Compared to Selexol, Rectisol has shown to be overall a better absorbent due to a multitude of factors. It has a higher diffusivity in both liquid and gas, a higher absorption capacity and a higher absorption rate [46]. There is however an issue with the operating conditions of Rectisol, in which its operating temperature is not ideal for the purpose of Carbon Dioxide capture. It like Selexol is also used for Carbon Dioxide rich gas streams.

Water* is a relatively weak absorbent. It does not have any outstanding qualities regarding absorption of Carbon Dioxide. Solubility of CO_2 decreases with increasing temperatures [16] There have been studies conducted that has shown water to be considerably worse than Selexol or Rectisol [46]. It has poor absorption rate, absorption intake, but saturates faster than Selexol and Rectisol. Some studies have compared tap water to distilled water, showing that distilled water has better absorbing qualities. It is however an absorbent that can be used as a reference and in the case of seeing experimentally how the absorption process changes according to variable parameters.

2.2.2 CHEMICAL ABSORBENTS

Chemical solvents exist within a range of different classes of chemicals, ammonia based, hydroxide based, amine based, and carbonate based being the most researched types for the purpose of Carbon Dioxide capture.

Monoehtanolamine, chemical formula $HOCH_2CH_2NH_2$, referred as MEA henceforth, is an amine-based chemical absorbent. It is a widely used and researched absorbent within carbon capture technologies and is used as a benchmark against other absorbents [11]. Costs wise it is cheap, but has high energy requirements in the regenerative step, making it costly depending on energy price. MEA is highly reactive towards Carbon Dioxide and is soluble to high amounts, but displays low selectivity, meaning that the risk of reaction with other particles remain high [11][43]. Additionally, it has a low absorption capacity. MEA has shown to be thermally unstable and corrosive, and with toxic byproducts. However, the technology to recover these byproducts is readily available [11][43].

Diethanolamine, also referred to as DEA, is an amine-based solvent. DEA is less-corrosive solvent than MEA, however it produces corrosive byproducts. It has high selectivity with slow reaction speed [8].

Ammonia solution, or aqueous ammonia, has been used for capture or removal of other acid gases, such as sulfur dioxide [11][43]. When used, it is operated at lower temperatures due to volatility, to avoid leakage of ammonia. The reaction rate for aqueous ammonia is slow but has high capture capacity.

Sodium hydroxide, NaOH, is an alkaline chemical compound that easily dissolves in water. It is readily available and cheap. Several studies have been made in regard to capture of CO_2 in

atmospheric air, meaning at very low concentrations of CO_2 [18][26]. NaOH is corrosive but does not display significant toxicity.

Potassium carbonate, K_2CO_3, has been a trending solvent in the field of Carbon dioxide absorption [31]. It does have some disadvantages such slow kinetics, while its main advantage compared to the highly used MEA is its environmental footprint and stability.

2.3 ULTRA-SONIC ATOMIZATION

In this section the concept of ultra-sonic atomization is discussed, as well as used for this work. Ultra-sonic atomization is a process in which high frequency vibrations, or ultra-sonic waves, are applied to a liquid generating waves on the surface of the liquid. From these waves, droplets are formed in the gas-liquid interface [20][33][42][48]. The formation of droplets has been investigated by many researchers and it has been found that it is possibly dependent on two mechanisms. Firstly, is the capillary wave theory and secondly the cavitation theory.

The capillary wave theory states that the droplet formation occurs at the surface of the generated liquid column from high frequency vibrations [13]. The droplets form from unstable oscillations that tear apart droplets at their peaks which leads to formation of mist due to high frequency.

The cavitation theory states that within the liquid phase, vapor bubbles are formed through the propagation of the ultra-sonic frequency waves. The bubbles are torn as it moves towards the liquid-gas interface creating shock waves which in turn generates ejected droplets at the surface.

There is no real definitive conclusion of which mechanism is said to happen, however it is widely accepted that both mechanisms play a role simultaneously, with either mechanism being dominant depending on various factors. Some research has been made on what these factors are that affect these mechanisms, going from the assumption that both cavitation and capillary waves occur simultaneously. It is found that at higher frequencies, at the range of MHz, the impact of cavitation lessens, this is due to a higher energy needed for cavitation to occur at higher ultra-sound frequencies [42] [44]. For cavitation to be a bigger factor to take into consideration at the MHz range, the power density of the transducer must be high.

This in turn also leads to a larger amount of droplets formed and a higher total surface area [42]. It has been found that by using Kelvin's equation, (Eq. 4)[36][39] in conjunction with the wavelength of the capillary waves, the mean droplet diameter can be estimated, (Eq. 5) [39].

$$\lambda = \left(\frac{8\pi\sigma}{\rho F^2}\right)^{1/3} \quad \text{(Eq. 4)}$$

$$D = 0{,}34\lambda$$

(Eq. 5)

In (Eq. 4), λ denotes the capillary wavelength, σ the surface tension, ρ the liquid density and F the frequency of the ultra-sonic transducer. For (Eq. 5), D is the mean diameter of the droplets and the factor 0,34 is a constant that has been estimated from collected data in a frequency range of 1kHz to 1MHz.

Other studies have reported that besides frequency, the droplet size can depend heavily on the liquid viscosity. A higher liquid viscosity would both suppress and enhance the cavitation effect. The higher viscosity of the liquid would act as a dampener to the shockwaves generated from erupted bubbles. This however creates a more localized effect, where the energy and temperature of the liquid increases due to the dissipated energy from the erupted bubbles [3][7][40], which also leads to a delayed formation of droplets, increasing the residence time. The resulting droplet size from the cavitation effect would end up being smaller. However, due to a suppressed cavitation effect from a smaller power intensity for this work, the influence of cavitation can be neglected.

It can thus be said that for the project, the outgoing assumption is that ultra-sonic atomization obeys the capillary wave theory, as the equipment at hand closely resembles that of what has been previously used for similar atomization studies.

Since the work handles ultra-sonic atomization of water, investigations has found that the droplet size distribution of atomized water ranges from 0,1um to 10um for a frequency of 1,7MHz. The number concentration of these droplets is found to be the highest at around 0,1um for tap water for frequencies 1,6MHz and 2,4MHz. Distilled water shows a peak at around 0,030um for frequencies above 1MHz, at 2,4MHz and 1,6MHz [42].

Regarding measuring of droplet size, it can vary due to multiple factors. One such factor is depending on whether one measures the droplet size at the onset or after a few moments [28]. The droplet size measured in this work should be that of less than a second after generation. Another factor of note is wave frequency. As frequency increases, the mean droplet size diameter decreases as the size distribution trends towards smaller droplets, at range of 80-300nm, this can be seen in Figure 1. Furthermore, in relation to droplet size, the density of the liquid affects the size. A higher density forms larger droplets [3].

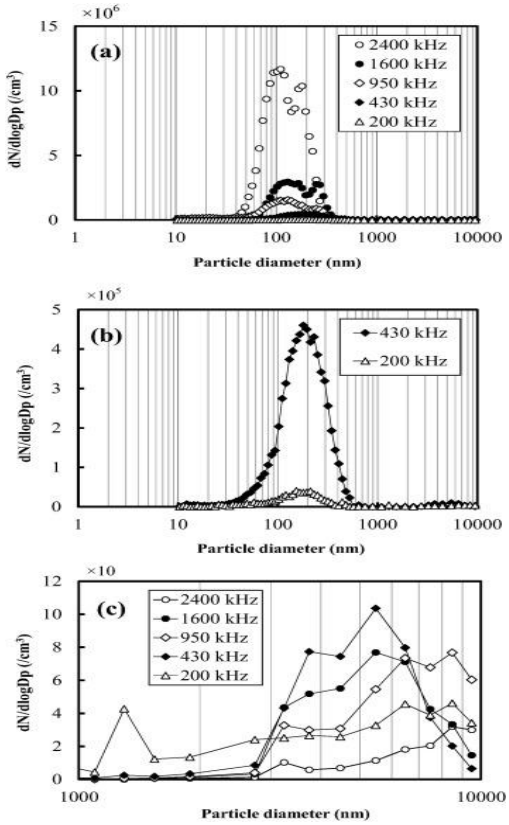

Figure 1 Size distributions of tap water mist generated at frequencies of (a) 200–2400 kHz, (b) 200 and 430 kHz, and (c) the size distribution from 1 to 10 μm. [42]

2.4 DROPLET/AEROSOL MASS TRANSFER MECHANISMS

Regarding the mechanisms involved in droplet absorption, there are differences in how a chemical absorbent and physical absorbent act. As it has been previously stated, physical absorption is diffusion dominated, and can be said to obey Henry's law. Mass transfer or the absorption process for physical absorption is dominated by two mechanisms. Depending on the presence of a solid nucleus and size relative to the droplet or the relative velocity between gas and droplet, internal circulation, or radial diffusion of the mass dominate [45].

Internal circulation is a mechanism that depends on the shear stress between the gas and the liquid surface. The gas is flown according to the streamlines of the droplet when within, the vortex [47]. With more time the concentration profile of the droplet has settled into the profile shifting away from the center. One half of the droplet would be deficient of the diffused gas along an oval shaped contour. [21][37][45][47]

Radial diffusion is controlled as the name states, diffusion along the radial axis of the droplet, obeying Fick's law. The diffused gas moves along the concentration gradient of the droplet, towards the least concentrated areas, the center. [45][47]

An increase in flow velocity of the gas increases the Reynolds number. When velocity is increased the impact of internal circulation becomes more apparent. Radial diffusion becomes less of a factor, and can be diminished for higher speeds, at above 1m/s.

Figure 2 shows the concentration profile of the upper half of a pure water droplet interacted with Carbon Dioxide through numerically methods at two different times [45]. These times corresponds to the convective time τ_c, denoting the time of when the gas and liquid has started its interaction, times a factor of 100 and 400 respectively, the latter time being at a saturated state. Convective time is inversely proportional to the Reynolds number. For the time of $100\tau_c$, the contour lower concentration contour is somewhat displaced from the center. This is due to a combined effect of both radial diffusion and internal circulation. However, it is observed that the contour shape is that of what is expected of radial diffusion. Next, as can be seen by the contours for the time of $400\tau_c$, the Carbon Dioxide concentration is not at its minimum along the center of the droplet. It does not display the shape of what is expected of radial diffusion, it is instead distorted. This is due to the effect of internal circulation, where the vortex is dominant in controlling the motion within the droplet.

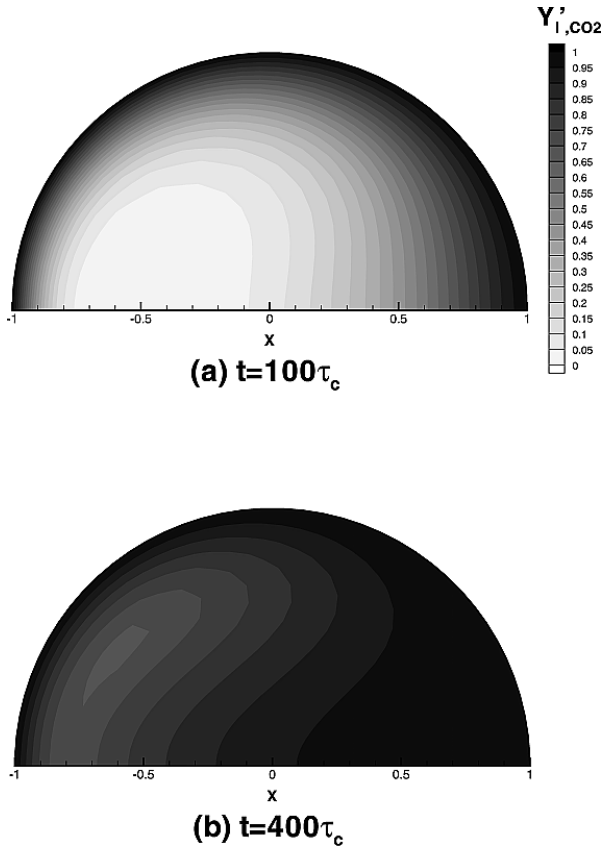

Figure 2 CO_2 concentration contours in the droplet at t = (a) 100 and (b) 400 τ_c (r_s/r_l = 0, Re_g = 1, and τ_c = 2.68 × 10^{-6} s). [45]

Internal circulation for an aerosol droplet with no solid nucleus of water dominates over other mechanisms to such an extent where it can be considered to be solely dominated by internal circulation if relative velocity between droplet and gas is high [47].

At the liquid-gas interface Henry's law is followed and the Henry's law constant for CO_2 absorption by water can be described by an equation seen in [46]:

$$c_{gs} = Hp_{ls}$$

(Eq. 6)

In this equation c_{gs} is the concentration between the gas and the liquid-gas interface, where $c_{gs}=c_{ls}$, the concentration between liquid and the liquid-gas interface. H is the henry's law constant in dimensionless form and p_{ls} is the partial pressure between liquid and the interface. Partial pressure is proportional to the concentration to its corresponding species, and as such a value for partial pressure can easily be assumed as being a percentage of the total pressure.

Solubility is closely linked to Henry's law constant [$Pa*m^3*mol^{-1}$], Henry's law constant for CO_2 in water in a temperature range of 272-433K can be seen in Figure 3 [5] comparing different models. A higher Henry's constant yields a lower solubility as temperature increases.

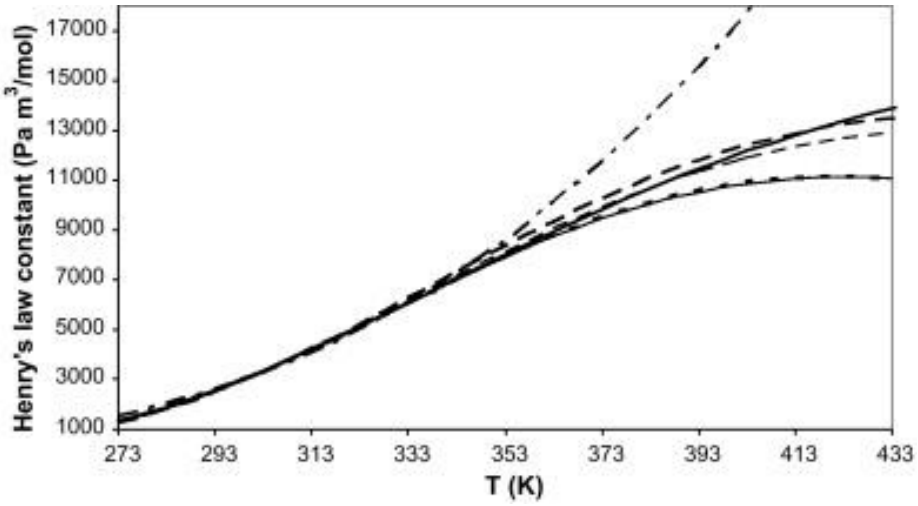

Figure 3 The Henry's law constant of CO2 in water. Comparison of the correlations by (…) Versteeg and van Swaaij, (—) Austgen et al, (–) Al-Ghawas et al., (— —) Jamal, (- - -) this work and (…) Carroll et al.. [5]

In general mass transfer is greatly affected by temperature and concentration ratio between the absorbent and its host. An increase in temperature decreases the mass transfer coefficient and an increase in the concentration ratio increases the coefficient [23].

3 METHOD

In this section the experimental setup is explained in detail, regarding its construction and the physics involved in their use, as well as detailing of the measuring instruments.

3.1 OVERVIEW

A schematic of the experimental setup is illustrated in Figure 4. As can be seen, it consists of various parts. The gas flows in through a series of sewage pipes, where it is blended with carbon dioxide, as can be seen at 1). After flowing through the pipe system, the gas enters a mist chamber, seen at 2). In this chamber mist is generated through ultra-sonic transducer and carbon dioxide within the gas is absorbed by mist droplets. From the mist chamber, the gas reaches another pipe, seen in 3), which can be called the transition pipe that leads to the disc stack centrifuge separator. The transition pipe is also where particle sizes are measured. In the disc stack centrifuge, seen in 4), the absorbed carbon dioxide is separated from the bulk gas, ending with the exhaust gas having a lower concentration of carbon dioxide. The exhaust pipe is seen in 5) and this is also where outlet CO_2 concentration is measured. The three main parts of the setup; 1) inflow piping, 2) mist chamber and 3) disc stack centrifuge, are further examined and explained in upcoming sections.

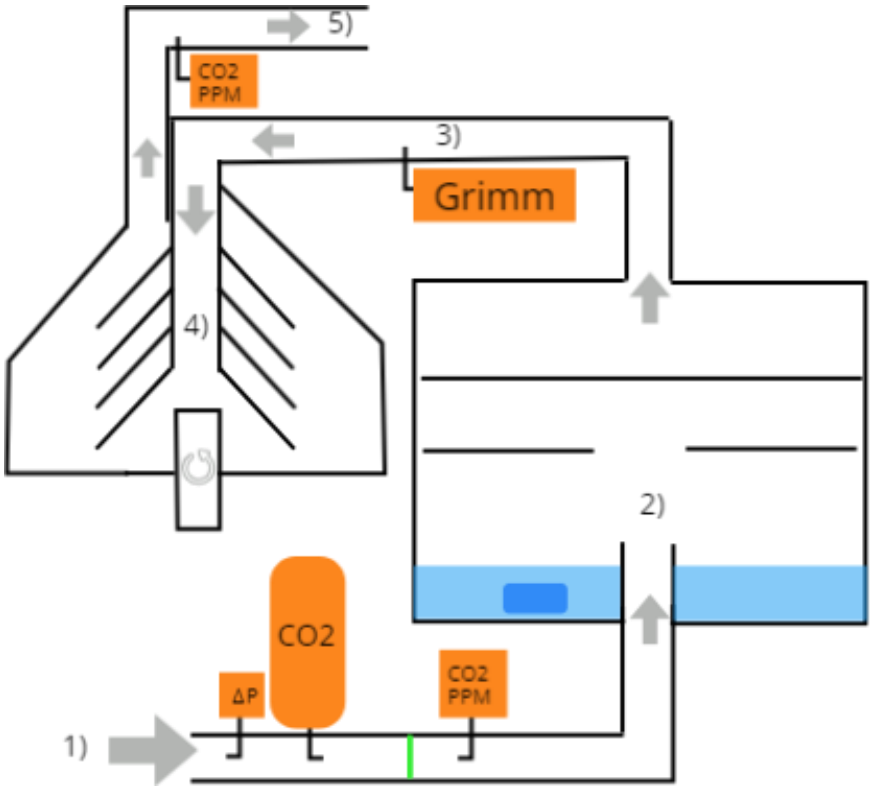

Figure 4 Schematic of the experimental setup. The numbers denote different parts and processes of the system. 1) is the gas inflow piping system, 2) is the mist chamber, 3) is the transition pipe, 4) is the disc stack centrifuge and 5) is the exhaust pipe.

3.2 ANALYSING INSTRUMENTS

The analyzing instruments that are used in the setup are the following:

- GRIMM AEROSOL and accompanying software
- CENTER 512 CARBON DIOXIDE (CO_2) METER and accompanying software
- 2x SENSIRON CARBON DIOXIDE SENSOR
- 2x AIRFLOW METER TSI
- MANOMETER WITH PRANDTL-PITOT TUBE
- pH MEASURING PEN and 7pH buffer solution

Grimm AEROSOL is a particle size measuring instrument. It can detect particles in a wide range of sizes; 0.28-10µm. It also able to measure total particle weight and count in different size ranges. To properly use this instrument, accompanying software is used. Previously it had been investigated that the size distribution would range within 80-300nm of droplets, it is possible for there to be a sizable number of droplets that are not registered.

CENTER 512 is a Carbon Dioxide measuring device. It can measure Carbon Dioxide concentration in the surrounding environment. It is also able to measure relative humidity and ambient temperature. There are various settings in this device, that allows measurement of CO_2 concentration that is time weighted or average weighted. This device has a visible LCD screen that can display the current CO_2 concentration. It also has accompanying software. The device can be used without software, so no connection between it and a PC is required during its operation, as it has a real time data storage function.

The Carbon Dioxide meters is located inside an airtight vessel which is connected to the initial piping through a tube and an air flow rate meter. This is to ensure that minimal loss of air as it is collected into the vessel. Two vessels were used. One connected with the initial piping near the inlet and one near the outlet gas. The gas is sampled in isokinetic condition within these vessels.

FLOW METER TIS is a simple instrument used for measuring the air flow rate. It is completely manual and does make use of any analogue instruments. It is therefore necessary to have to read the flow rate in real time. It is used to adjust the flowrate of Carbon Dioxide. Due to the instrument being used for air, the Carbon Dioxide flowrate can be calculated by a pair conversion equations from air to Carbon Dioxide, where their densities are known.

A manometer designed for air flow is used to measure the inlet differential pressure through the use of a Prandtl-Pitot tube.

A pH measuring pen is obtained from Labmate. This pen shows pH between 0-14pH in 0.01 increments. The accuracy is said to be at 0,05pH between 6-8pH and 0,1pH outside that range. The pen is obtained along with a buffer solution of 7pH in order to calibrate the pen.

3.3 FLOW PIPE AND CARBON DIOXIDE INJECTION SYSTEM

The experimental setup begins with the inlet pipe. A schematic of the piping setup can be viewed in Figure 5. The is pipe is meant for sewage purposes and is made of Polypropylene.

The piping consists of two connected pipes of 1 meters each in length, making the total pipe length 2 meters. The pipe has both an inner, d_i, and an outer diameter, d_o; 45.8mm and 50.8mm respectively.

For applying Carbon Dioxide separately and measuring purposes the pipe has been drilled with holes at different locations. The first drilled hole is located at 500mm from the inlet, 2) in the figure. The purpose of this hole is to measure the inlet flow rate by the use of a Prandtl-Pitot tube, in which differential pressure is measured.

The second hole is located 750mm from the inlet, 3) in the figure. From this hole, Carbon Dioxide is applied through tube connection.

The purpose of the third hole, 5), is to measure the Carbon Dioxide concentration of the gas flow. It is located 1250mm from the inlet. The setup for the Carbon Dioxide concentration measurement has been previously detailed.

In the middle, where the 2 pipes connect, at one meter, a porous material had been inserted, as seen in 4) in the figure. This is to ensure that the gas is able mix with the injected Carbon Dioxide. The size of this material is kept constant throughout the experiment, it is chosen due to being thick enough to not significantly hamper the airflow of the system.

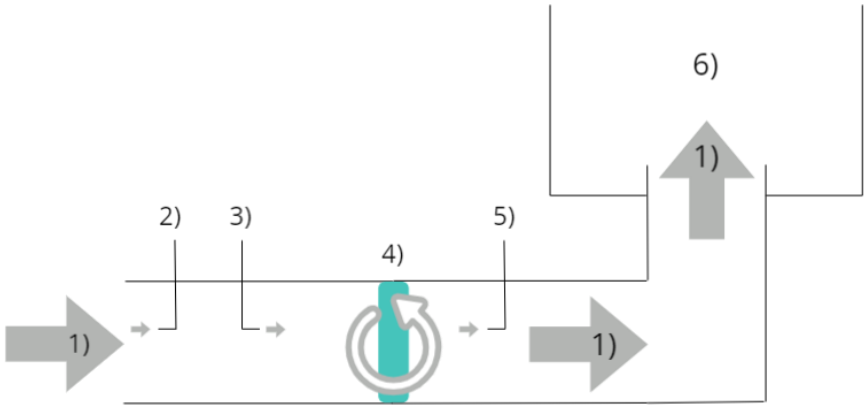

Figure 5 Schematic of the piping system. The numbers denote different parts of the system and processes. 1) is the flow direction, 2) is the Prandtl-Pitot tube, 3) is the CO_2 inflow into the system, 4) is the porous material used for gas mixing, 5) is the sampling of the gas mix for CO_2 measurements and 7) is the mist chamber.

In order to calculate the theoretical Carbon Dioxide concentration after mixing, as a reference to the displayed concentration from the CO_2 meter, a number of parameters need to be known, starting by the use of (Eq. 7).

$$Q_{air} = U \times A = U_{air} \times (\pi r_i^2)$$

(Eq. 7)

Q is the volumetric flow rate of the inlet gas; U is the bulk velocity and A is the cross section of the pipe. U is measured by the use a Prandtl pipe in conjunction with a manometer where the differential pressure can be measured.

In order to calculate the volumetric flow, air velocity needs to be calculated, which can be done by (Eq. 8).

$$U_{air} = \sqrt{2 \times \Delta p / \rho_{air}}$$

(Eq. 8)

Δp is the difference between the static and dynamic pressure within the tube.

In order to calculate the flow velocity of the added Carbon Dioxide, the following form of Bernoulli's equation, (Eq. 9), can be used:

$$\rho_{air} \times U_{air}^2 = \rho_{CO_2} \times U_{CO_2}^2$$

(Eq. 9)

Due to the cross section being equal for both cases, the flow velocity can be exchanged with the volumetric flow rate shown in (Eq. 10).

$$\rho_{air} \times q_{air}^2 = \rho_{CO_2} \times q_{CO_2}^2$$

(Eq. 10)

From which the added Carbon Dioxide volumetric flow rate can be calculated as shown in (Eq. 11):

$$q_{CO_2} = \sqrt{(\rho_{air} / \rho_{CO_2})} \times q_{air}$$

(Eq. 11)

The mixed Carbon Dioxide concentration, (Eq. 12), can thus be calculated:

$$C_{mix} = \frac{C_{in} Q_{air} + C_{100} q_{CO_2}}{(Q + q_{CO_2})}$$

(Eq. 12)

C_{mix} is the mixed Carbon Dioxide concentration; C_{in} is the Carbon Dioxide concentration from the inlet flow and C_{100} is around 1 as it is the added pure Carbon Dioxide concentration. The relationship between the system airflow with varying CO_2 inflow can be seen in Figure 6, and CO_2 inflow with varying system airflow in Figure 7.

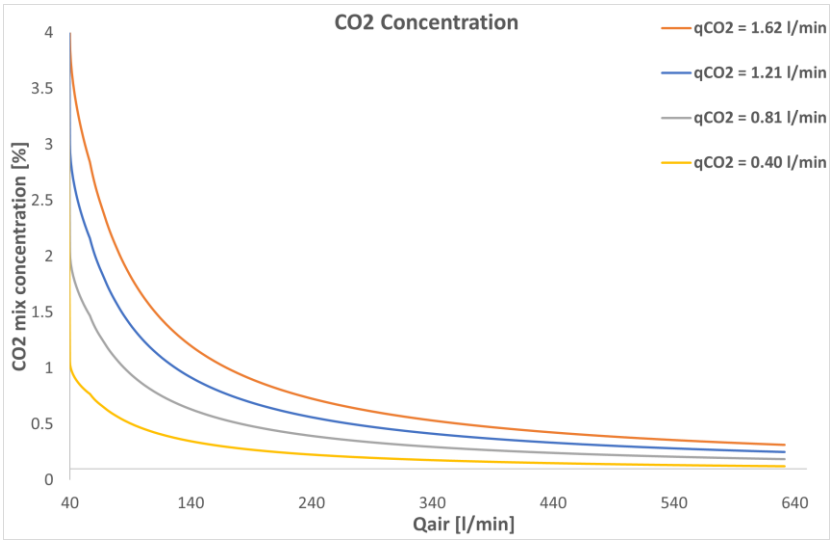

Figure 6 The mixed CO_2 concentration as a function of the inlet flowrate, for different CO_2 inflow rate.

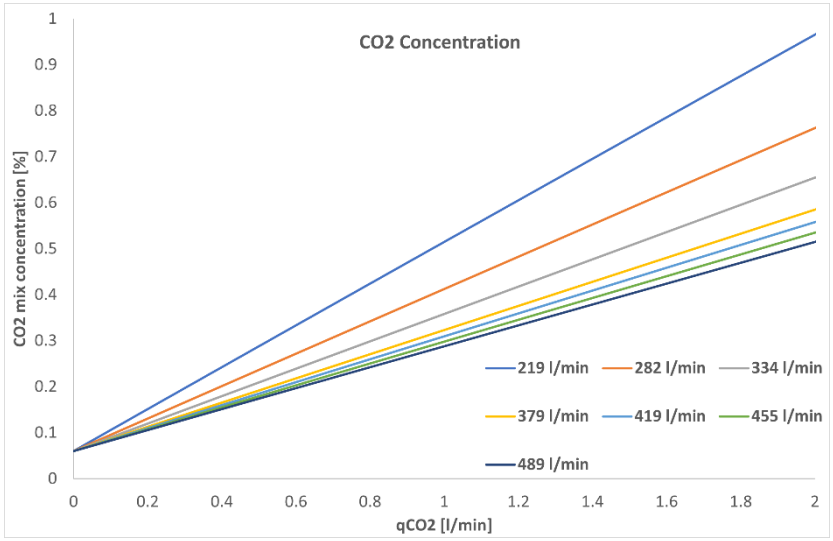

Figure 7 Theoretical CO_2 mixed concentration as a function of the inflow of Carbondioxide before mixing.

A fraction of the inlet flow is measured when measuring the Carbon Dioxide concentration, about 2-2.5l/min of the mixed flow is sampled, seen at 5) in the figure. This fraction is dependent on the inflow. For the outflow, this fraction ought to be around the same amount.

3.4 MIST CHAMBER AND ULTRA SONIC TRANSDUCER

Following the pipes, the mist chamber is the next step in the Carbon Dioxide separation process. The mist chamber consists of a chamber vessel, a commercial ultra-sonic transducer with 5 membranes from Pondteam, as well as 2 metal discs. A schematic of the mist chamber can be seen in Figure 8.

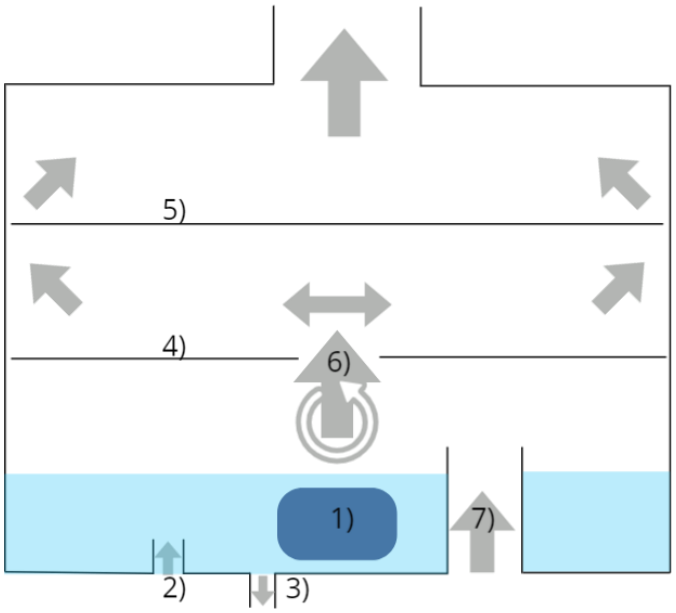

Figure 8 Schematic of mist chamber used. The numbers denote different parts and processes in the system. 1) is the ultra-sonic transducer, submerged in liquid, 2) is the liquid feed, 3) is the liquid drain, 4) is Disc A, 5) is Disc B and 6) is the mist mixed with the gas mix and 7) is the gas mix.

The vessel for the generated mist is made of plastic and has a metallic bottom and lid. The lid has a hole that protrudes outwards and is connected to a pipe. The metallic bottom has several holes. These holes have been purposed into inflow of liquid for mist generation, outflow of liquid to empty the vessel if necessary for cleaning and inflow of the gas blend from the initial pipe. For the experiments, the vessel is filled with 3.5-4 liters of solvent liquid.

The ultra-sonic transducer is the key component for the mist generation. It is a transducer with 5 membranes and has to be submerged to be operational. The frequency is unknown, however other similar transducers in other reports have shown to be 1700kHz. Due to the number of membranes, the transducer is posed to be a more powerful variant. It can be assumed that this transducer is of a similar frequency. The transducer has a water consumption rate of 400ml/hour according to manufacturer notes.

Regarding the discs within the mist chamber, the purpose of these discs is to ensure a better gas blend and lengthier path for the gas to have contact with the generated mist. The discs are stacked in an alternate fashion:

Disc A – Disc B

Both discs have the same size; however, Disc A has a hole cutout at the center as mentioned earlier. This setup is to allow the mist blend to flow for a longer time, where the flow starts as divergent to convergent to divergent and finally convergent as the mist flows into the next step.

Before the gas and mist blend enters the disc stack centrifuge, it is flown through the transition pipe mentioned earlier. This pipe has a hole, which is used for measuring particle size with GRIMM instrument.

3.5 WATER

For the experiment, water is used as an absorbent on its own and as a solvent, specifically tap water. Tap water unlike distilled water is not pure water. It contains impurities, of either solid, liquidous, or gaseous kind.

The solubility of CO_2 in water can be calculated by using the Henry's law solubility constant, H_s^{cp} and multiplying it with the partial pressure of CO_2. The constant, with a temperature dependance, can be calculated by (Eq. *13*) [41][46]:

$$H_s^{cp}(T) = H_s^{cp} \times \exp\left(\frac{\Delta H}{R}\left(\frac{1}{T_s} - \frac{1}{T}\right)\right)$$

(Eq. 13)

H_s^{cp} is the constant for a temperature, T_s, of 298.15K, and amounts to 0.034 M/atm and $\Delta H/R$ is 2400 K. Since the experiment is done at a temperature around 20C°, the temperature is set to 293.15 K, which leads to a Herny Solubility of 0.0296 M/atm. The system can be assumed to be operated under 1 atm.

Depending on the partial pressure, the solubility varies linearly as seen in *Figure 9*, where a higher temperature yields lower solubility.

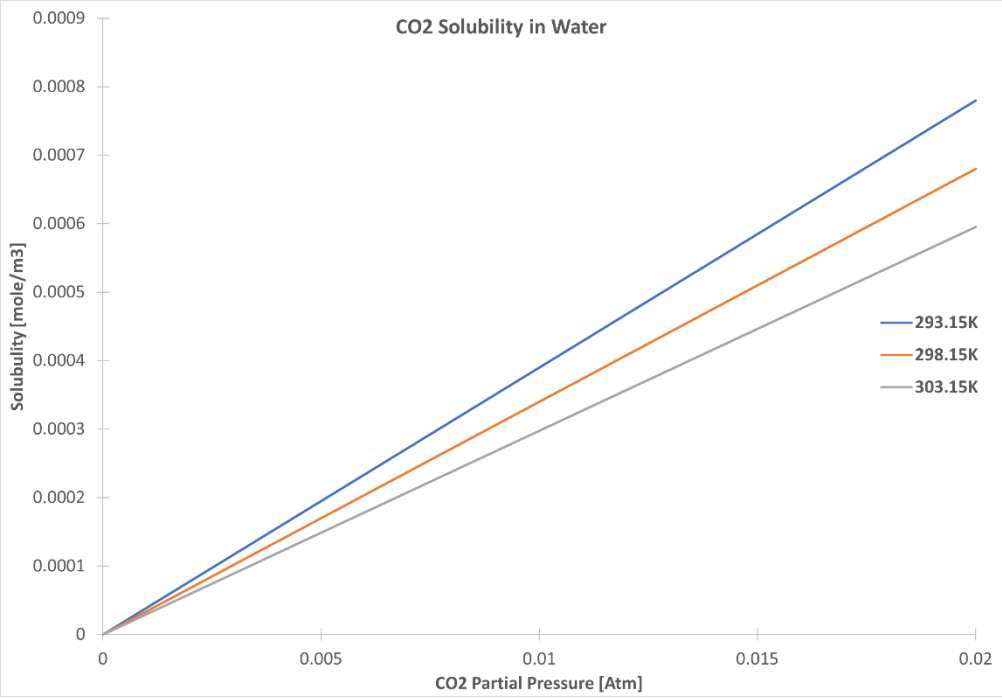

Figure 9 Solubility of CO_2 in water as a function of partial pressure of CO_2 for temperatures between 293.15-303.15K.

Additionally, since the water consumption of the ultrasonic transducer is 400mL/h a theoretical maximum of carbon absorption can be calculated.

The maximum molar and mass ratio that is employed, between CO_2 and Water, is 0.85 and 2.08 respectively, at CO_2 of 2%.

3.6 SODIUM HYDROXIDE

Sodium hydroxide, NaOH, is used as an absorbent aerosol. Commercial NaOH, in the form of small pellets used for cleaning sewage, with a supposed purity of 99% according to manufacturer information, is dissolved in water to make a solution, where the pH is kept between 9.0-9.5pH and 11.0-11.5pH. For lower pH, a pH measuring pen is used due to weighing the pellets proved to be difficult at very low amount, in the range of mg.

The pellets were weighed for solutions over 13pH, since the pen could not be used due to being one-point calibrated, at 7pH. The water that is used for the solution is not distilled or deionized. This means that this relation is not precise but instead approximated. Between 9.0-9.5pH and 11-11.5pH the solution concentration of NaOH corresponds to approximately 0.00001-0.000032M and 0.001-0.0032M NaOH respectively. Since NaOH is consumed at a constant rate by the mist generator, one can assume that this relation is constant throughout the whole process, up to a certain amount of time which is not surpassed.

The reaction between the gas and solution can be described as shown between reactions (Eq. 14)-(Eq. 18) [18][30][34]:

$$2NaOH_{aq} + CO_{2_{(g)}} \Longrightarrow Na_2CO_{3_{aq}} + H_2O_{(l)} \quad \text{(Eq. 14)}$$

$$Na_2CO_{3_{(aq)}} + H_2O_{(l)} \rightleftharpoons 2NaHCO_{3_{(aq)}} \quad \text{(Eq. 15)}$$

$$CO_{2_{(aq)}} + OH^-_{(aq)} \rightleftharpoons HCO^-_{3\,(aq)} \quad \text{(Eq. 16)}$$

$$HCO^-_{3\,(aq)} + OH^-_{(aq)} \rightleftharpoons CO^{-2}_{3\,(aq)} + H_2O_{(l)} \quad \text{(Eq. 17)}$$

$$NaOH_{(aq)} + CO_{2_{(aq)}} \Longrightarrow NaHCO_{3_{(aq)}} \quad \text{(Eq. 18)}$$

In (Eq. 16) and (Eq. 17), the ionic reactions can be seen. These two reactions happen simultaneously and are both reversible. Hydroxide ions are continuously consumed during the

absorption process, leading in essence to a depletion of NaOH, thus NaOH is limited in comparison to CO_2, the resulting reaction can be seen in (Eq. 19):

$$NaOH_{(aq)} + CO_{2_{(g)}} \Longrightarrow NaHCO_{3_{(aq)}}$$

(Eq. 19)

As 2 moles of NaOH reacts with 1 mole of Carbon Dioxide, 1 mole of sodium carbonate, Na_2CO_3 is produced. Due to the mass ratio between one mole of both compounds being almost 1:1, the mass ratio for this reaction is approximately 2:1. For this experimental procedure the molar flow rate between CO_2 and NaOH is at its most around 170, meaning that this ratio would increase with time due to no additional injection of NaOH in the mist chamber.

In an experimental study it is found that the yield, in other words the measured absorption compared to the theoretical, ranges between 0.8442 to 1.0477 depending on the concentration of the NaOH solution, between 1-5% [34], the study did not experiment on separation of CO_2. The experiment is conducted at a Carbon Dioxide concentration of 30% with NaOH solution at 1-5% concentration, where the solution amount is depleted over a longer period of time, up to 2 hours, as CO_2 is continuously fed. This can be seen in Figure 10. As is expected, the higher concentrated solution takes more time to be fully depleted, however the time for outlet concentrations of CO_2 drastically reverting to the feed concentration does not differ as much. The higher concentrated solution takes longer to completely deplete and for CO_2 to no longer be absorbed.

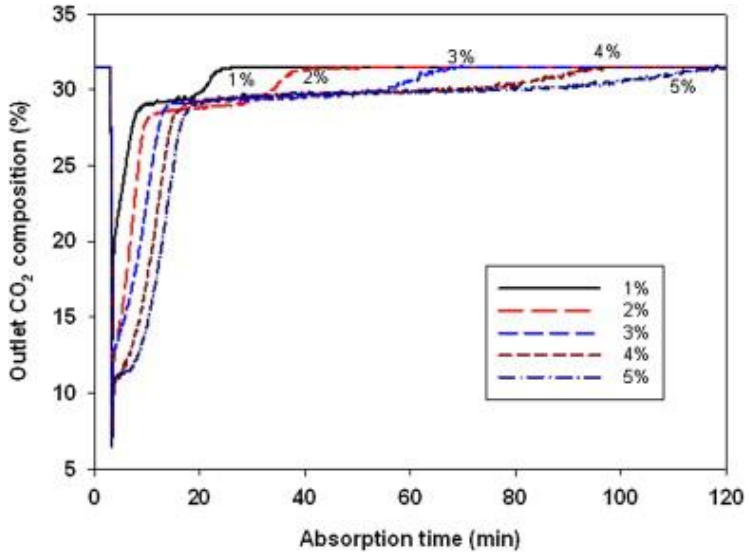

Figure 10 Absorption behavior of CO2 in each NaOH solution according to absorption time. [34]

Due to limitations of the present equipment in this study, testing at these conditions for a disc stack centrifuge is not possible, as there is no measuring device available to measure Carbon Dioxide concentrations above 3% for this task at reasonable costs, and the working

environment is not deemed suitable for concentrations of such an amount of sodium hydroxide.

3.7 DISC STACK CENTRIFUGE SEPARATOR

The disc stack centrifuge is the main instrument for the separation of absorbed Carbon Dioxide particles. It also works as a pump for the whole system, due to its high rotation speed. The rotation of the centrifuge can be varied through a frequency converter. The effect of the rotation speed can be seen through the use of Prandtl-Pitot tube and an accompanying flowmeter or manometer as previously mentioned in the pipe section. A schematic of a disc stack centrifuge can be seen in Figure 11, however the used disc stack is not 1:1 in its appearance to the schematic.

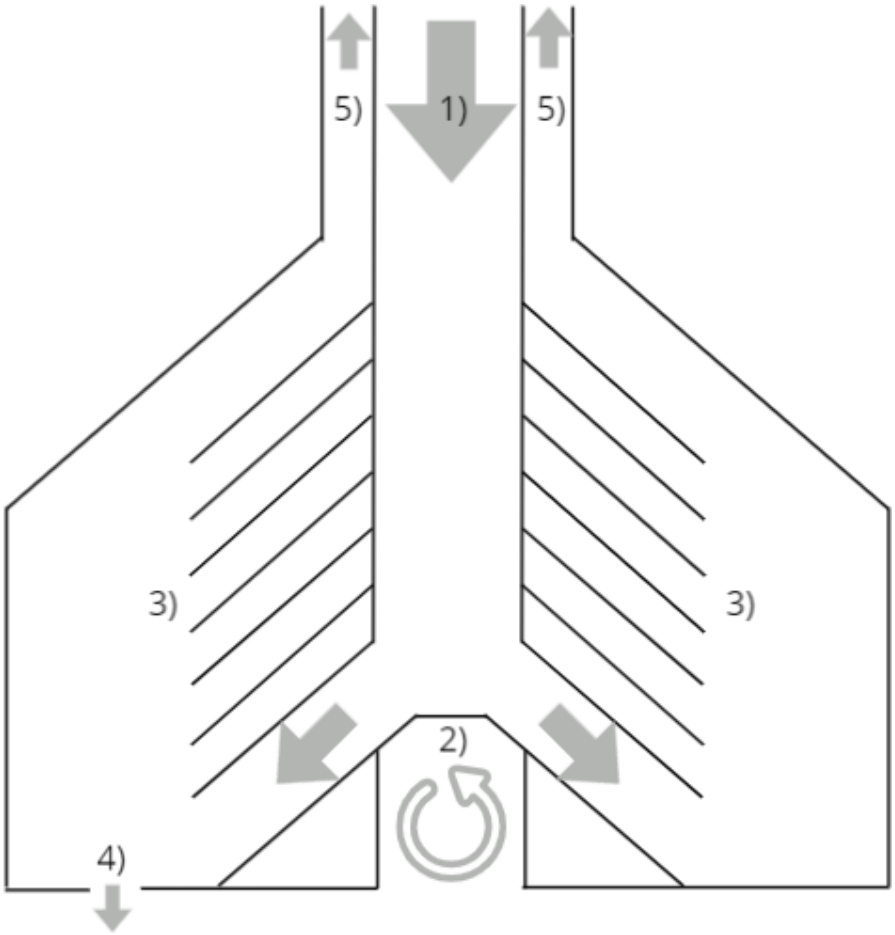

Figure 11 Schematic of a disc stack centrifuge. The numbers denote different parts and processes in the system. 1) is the direction of flow from the mist chamber, 2) is the rotor, which rotates the disc stack, 3) is the disc stack, 4) is the discharge of the separated material and 5) is the outflow of the cleansed gas.

The centrifuge is a self-produced lab scale model of 3Nine, that has previously been used for other applications such as separating oil droplets in workshop environments.

Two rotation speeds were used on the frequency converter, 61.95 and 82.95rpm. Converted to angle velocity their respective speeds were ω_1=389.24rad/s and ω_2=521.19rad/s. In order to calculate that settling area of the disc stack, (Eq. 20) is used from which (Eq. 21) is brought from, by the omission of the settling velocity. It can be derived by either using the disc stack dimensional parameters and angle velocity or by the knowledge of the volumetric throughput, Q, divided by the gravitational velocity of a particle, v_g. The equation for the gravitational velocity of a particle is seen in (Eq. 22). The density difference, $\Delta\rho$, denotes the difference in density between the two phases in the particle, in this case the aerosol of NaOH solution or aerosol of tap water and air mix.

$$Q = \frac{2}{3g}\pi n\omega^2 cot\varphi(R_o^3 - R_i^3)v_g = A_e v_g \quad \text{(Eq. 20)}$$

$$\frac{2}{3g}\pi n\omega^2 cot\varphi(R_o^3 - R_i^3) = A_e \quad \text{(Eq. 21)}$$

$$v_g = \frac{d^2\Delta\rho}{18\mu}g \quad \text{(Eq. 22)}$$

Due to the limited amount of liquid that is vaporized, there is around 3.5l of water or NaOH solution in the mist chamber and a fraction of that is vaporized per minute, it can be assumed that the input airflow barely changes when in contact with the mist, so it can be assumed constant.

From the centrifuge there is a drain in which the separated particles are drained by gravity, seen at 4) in the figure. The bulk after separation flows out as seen at 5) in the figure.

3.8 EXPERIMENTAL PROCEDURE

The experimental procedure is started by first turning on the separator, which acts as a gas fan for the Carbon Dioxide measurement vessels and subsequently turning on the CO_2 injection from the gas tube. For each measurement, due to the reaction time of the sensors, a few minutes had to pass in order for the sensors to stabilize, in conjunction with time needed for the vessels to be filled. Additionally, for each measurement cycle the Ultra-sonic transducer is also turned on.

3.8.1 DESCRIPTION OF EXPERIMENTAL TEST RUNS

A number of parameters for the experiment were varied. These include the regulation of rotor speed, CO_2 inflow rate and NaOH concentration.

Rotor speed is regulated by adjusting the frequency by turning a knob. Two different speeds were used during the measurements. Lower speeds were measured at first, but it would not yield any measurable results due the mist not flowing through the separator because of the low airflow, leading to a larger condensation rate withing the mist chamber.

The flow is regulated by a regulator connected to a tank of CO_2. Carbon Dioxide inflow rate between 0.4-1.6 L/min is measured by observing a TSI Airflow meter. Above 5 L/min, the inflow rate is observed through the embedded flowmeter on the regulator.

NaOH concentration is varied and measured by measuring the pH of the solution for lower concentrations of NaOH, for high concentrations of NaOH the weight of NaOH pellets were weighed and then dissolved in water. While the water is not of pure character, it is assumed that its weight is that of pure water.

3.8.2 UNCERTANTIES

The experimental procedure procures several uncertainties. One of the major uncertainties is the CO_2 inflow through the regulator. There is a tendency of the regulator not being stable for lower inflow, as such the measured concentration is dependent on these fluctuations.

In regard to the state of the water used, the municipality of Nacka, the base of operations for this work, has stated that the pH of its tap water is about pH 8. This would yield an uncertainty of pH between 0 and 1.

4 RESULTS AND DISCUSSION

4.1 CO_2 SEPARATION BY MIST

In Figure 12 and Figure 13 the CO_2 concentration against time can be seen, as well as the relative humidity, for CO_2 exposed to mist at different times. The relative humidity is shown in order to give grasp on when mist generated. The mist generation corresponds to an increase in the relative humidity, RH, and dips in RH corresponds to when the mist generation is turned off. CO_2 inflow conditions corresponds to that of 2l/min, 1.5l/min and 1l/min CO_2 mixed with air of higher and lower flowrate.

In Figure 12, between the time of 11:06 and 11:41 the battery of the sensor had been depleted. There were however no active measurements done during this short period of time. In Figure 13 between the time 11:40 and 12:40 was a break and data shown there only shows the outflow concentration with the separator on without any mist generation and 0l/min CO_2 inflow. RH measurements are taken from the Centertek CO2 sensor. There is no observable CO_2 separation, when comparing the status of when the mist generation is off and on. Some dips are shown, around 10:40 and 11:00 however it is not possible determine if it is due to the mist generation or the CO_2 inflow having sudden disturbances, which has been seen various times during the entire experimental phase.

In regard to the sensor, an aspect to note is the delay of the sensor. Since it takes around 2 minutes to empty or fill the vessels, it should take approximately the same amount of time for the CO_2 concentration measurements to stabilize if there are no changes in the system.

The duration of each mist measurement was approximately 10 minutes. Larger changes in the system, as in the mixed CO_2 concentration and the relative humidity, are quickly registered, as can be seen in how concentration and RH values quickly increase, although it takes additional time for those values to stabilize. However, the reverse scenario, large changes in the system by decrease of CO_2 and RH, takes a longer amount of time to stabilize.

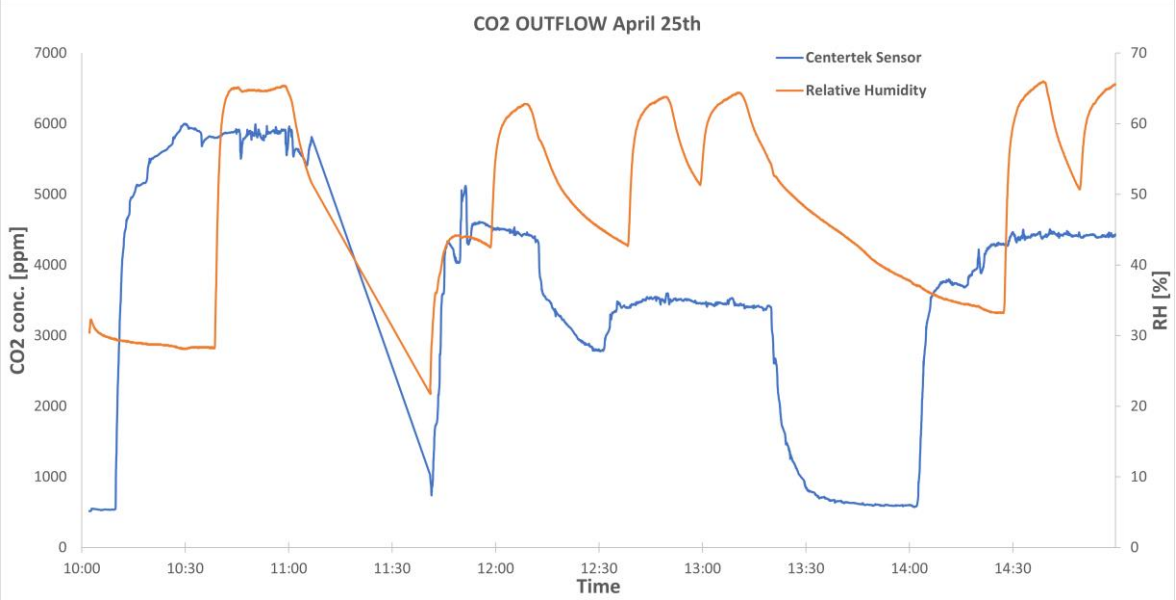

Figure 12 Outflow CO_2 concentration in ppm and relative humidity plotted in % against time, for one sensor. Tap water was used as aerosol for this measurement period. Blue corresponds to the CO2 concentration, and orange the relative humidity.

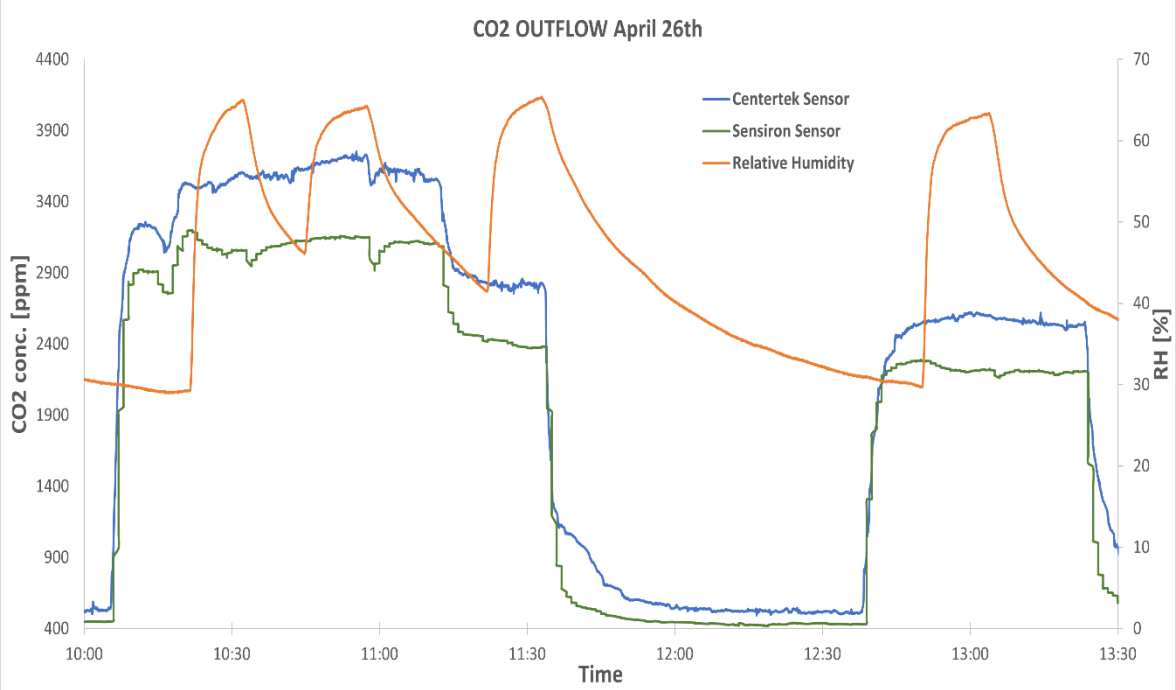

Figure 13 Outflow CO_2 concentration in ppm and relative humidity in %, plotted against time, for two different sensors. Tap water was used as aerosol for this measurement period. Green and blue corresponds to the CO2 concentration, and orange the relative humidity.

In Figure 14 the CO_2 concentration is measured against time as mist switched on and off for two different sensors. The difference between this figure and, 12 and Figure 13 is that the mist

has been infused with NaOH. The NaOH concentration was equivalent of 9-9.5pH and 11-11.5pH and the CO2 inflow was that of 2l/min. Between the time of 10:00:11:33 the pH was on the lower end interval. The higher pH interval was measured between 13:00-14:00. Dips are observed at numerous points, however they do not necessarily correlate to the presence of NaOH, as there are some increases during mist generation.

The figure also displays some notable differences in the CO_2 concentrations between the two sensors, however the difference appears to be consistent between any increases or decreases in CO_2 inflow and can be said to be a difference of accuracy, reaction time and software between them.

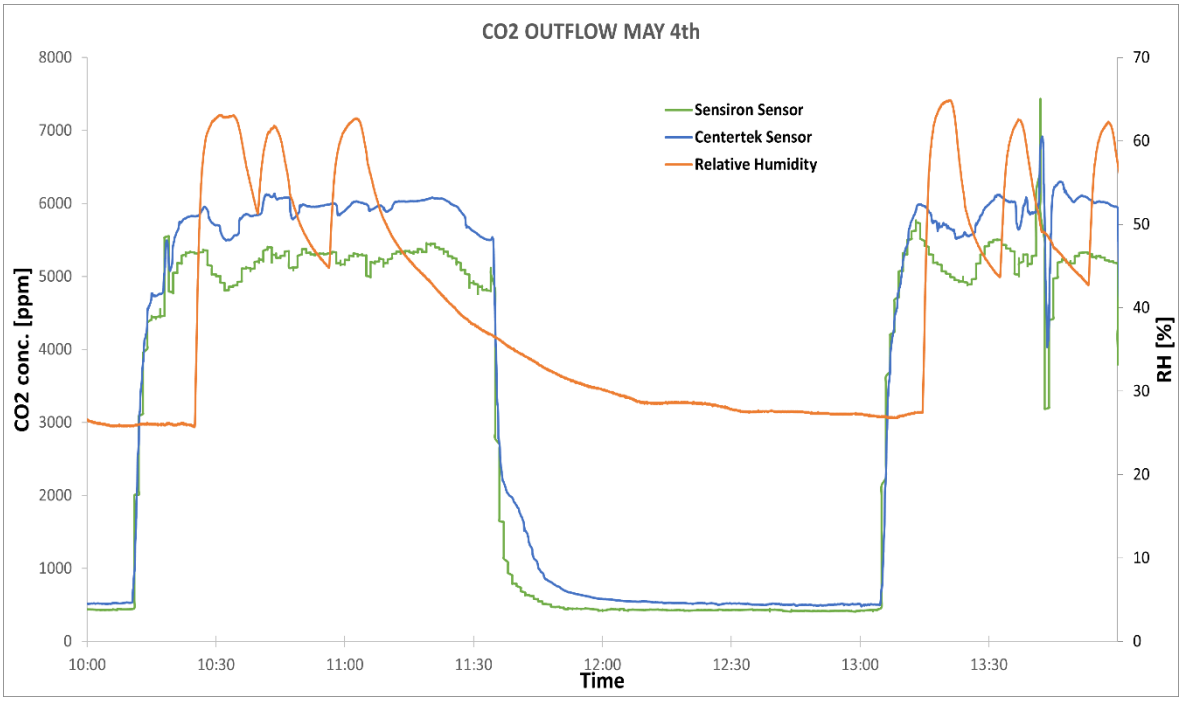

Figure 14 Outflow CO_2 concentration in ppm and relative humidity in %, plotted against time, for two different sensors. NaOH concentration between pH 9-11.5 was used aerosol for this measurement period. Green and blue corresponds to the CO2 concentration, and orange the relative humidity.

In Figure 15 and Figure 16, CO_2 concentration was measured for a much higher initial CO_2 concentration than previously, as well as a NaOH solution of approximately 0.25M. This measurement was the most extreme of any that has been done, due to the large increase in both CO_2 and NaOH. The figures do not show any notable changes in CO_2 concentration as a result of the mist. This can be partly answered by a noticeable instability in the CO_2 was observed. Due to no noticeable changes in concentration for this measurement, it can be assumed that any changes from earlier were due to instability of the CO_2 inflow. For the times when the mist was turned on, the duration of the mist generation was around 10 minutes, in which afterwards it was turned off for a similar amount of time.

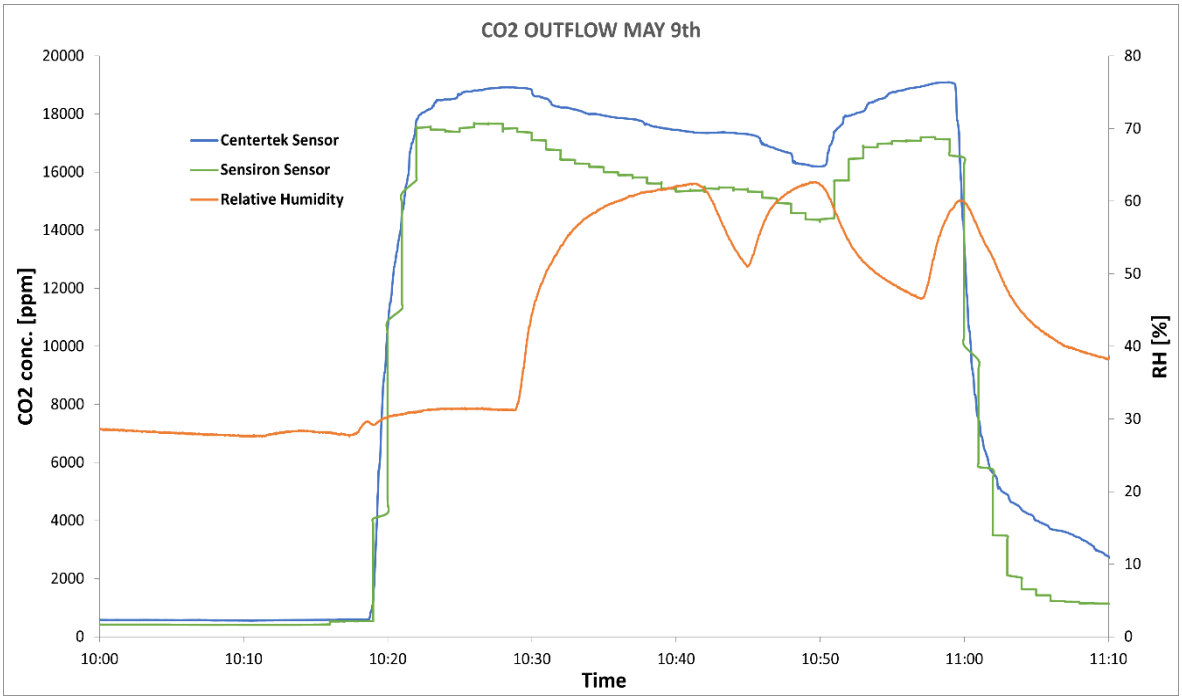

Figure 15 Outflow CO_2 concentration in ppm and relative humidity in %, plotted against time for two different sensors. 0.25M NaOH aerosol was used for this measurement period. Green and blue corresponds to the CO2 concentration, and orange the relative humidity.

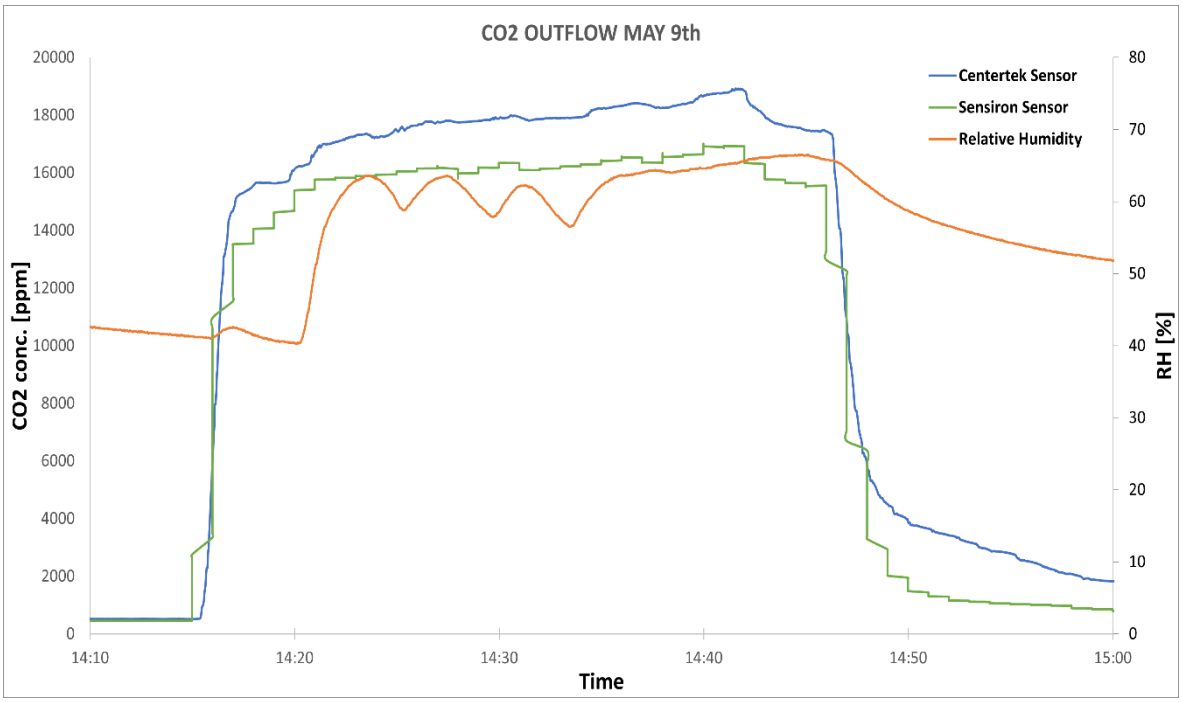

Figure 16 Outflow CO_2 concentration in ppm and relative humidity %, plotted against time for two different sensors. 0.25M NaOH aerosol was used for this measurement period. Measurements were done at an increased injection of CO_2. Green and blue corresponds to the CO2 concentration, and orange the relative humidity.

4.2 DISCUSSION OF CO_2 CONCENTRATION MEASUREMENTS

Separation with a sodium hydroxide solution turned out to not yield any satisfactory separation. Due to the instability of the CO_2 inflow, any notable increase or decrease in concentration cannot be determined by whether it is by absorption and separation or due to CO_2 inflow instability. NaOH was also very low in conjunction with the Carbon Dioxide concentration being low, where there is a lower total surface area for these particles to interact with each other. Other experiments and simulations have used higher concentrations of both solution and CO_2.

Due to this shortcoming, an increase in the carbon dioxide inflow was made, leading to the CO_2 concentration measuring around 1.5-2%. This was in order to see if any notable differences in capture was made to offset the smaller errors of lower CO_2 concentrations. However, an increase in concentration of CO_2 did not yield any notable results, and as such the decision to further increase the NaOH solution concentration was made, to that of around 1%wt NaOH, or 0.25M NaOH, which also did not yield any measurable separation results.

An explanation for this could be that the residence time of the mass diffusion and reaction time between the gas and solution is too short compared to the velocity of the system. The diffusion and reaction do not have enough time to complete before the separation step. The distance between system and piping between the mist chamber and separator is not long enough.

Another approach would be to decrease the velocity of the system, however in previous findings during preparations, it was observed that the mist did not flow through the separator well and the condensation rate of the mist was too high. This lead to a loss of water into the inflow pipe, where it partially blocked the inflow after a short amount of time. This was partly compensated by the removal of one disc in the mist chamber, which did lead to less water condensing into the inflow pipe. The reason for the water condensing into the pipe was because of the distance between the disc and the inflow pipe was small, droplets would immediately fall from the bottom of the disc into the pipe.

4.3 PARTICLE SIZE DISTRIBUTION

The particle size distribution of two different flows can be seen in Figure 17 and Figure 18 for water as an absorbent. As can be seen, the distribution is that of mass in micrograms per volume [$\mu g/m^3$] vs the particle size [µm]. The mass of droplets within the range of 5 microns proved to be the highest, in the cases of both lower and higher flow. The distribution appears to be mostly similar in both cases, in terms of their probability density value.

For higher flow, it appears that the Carbon Dioxide inflow of 1.5l/min is higher by a noticeable amount than that of 1l/min and 2l/min. An explanation for this can be that the Grimm Aerosol had issues with measuring at some point the size during the measurement because of high humidity within the tubes and droplets condensing, thus blocking the sampling inflow, that connected Grimm to the measuring spot. For the lower flow, the higher Carbon Dioxide inflow is observed to be in parity or higher than its lower Carbon Dioxide inflow counterparts.

In regard to the differences between the three different Carbon Dioxide inflow, there is no definite conclusion to make in regard to the absorption of Carbon Dioxide of the water droplets, except that for the two higher Carbon Dioxide flows, the droplets weigh more in most of the size range, by very small margins. Whether is proof of absorption or not cannot be concluded.

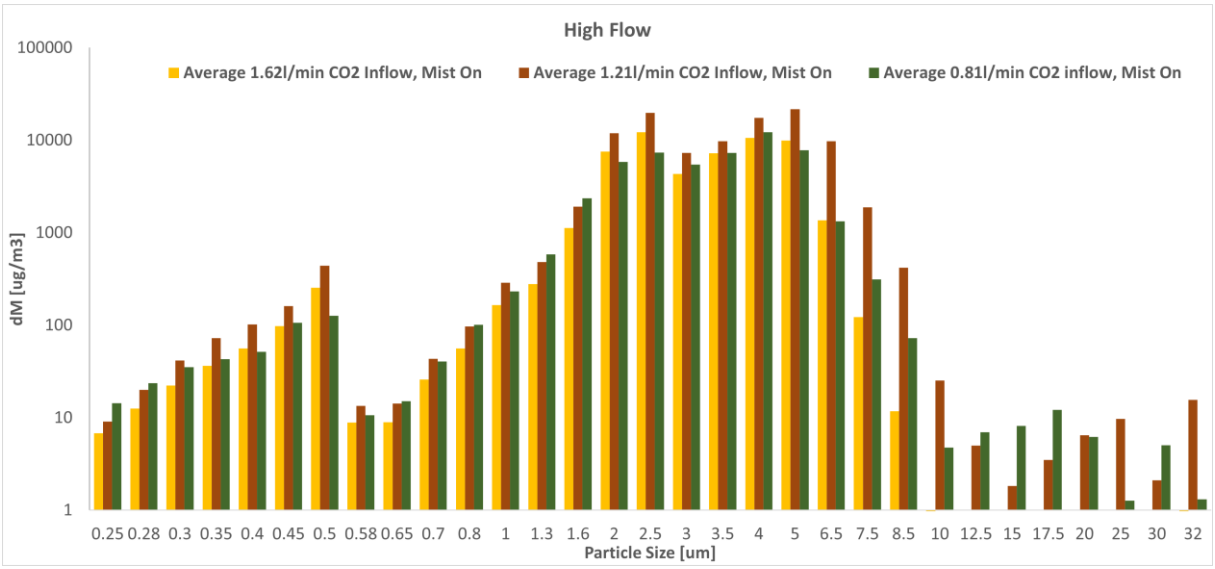

Figure 17 Particle distribution by mass of water aerosol mixed with Air infused CO_2. The air flow is high. Measurement was done before separation.

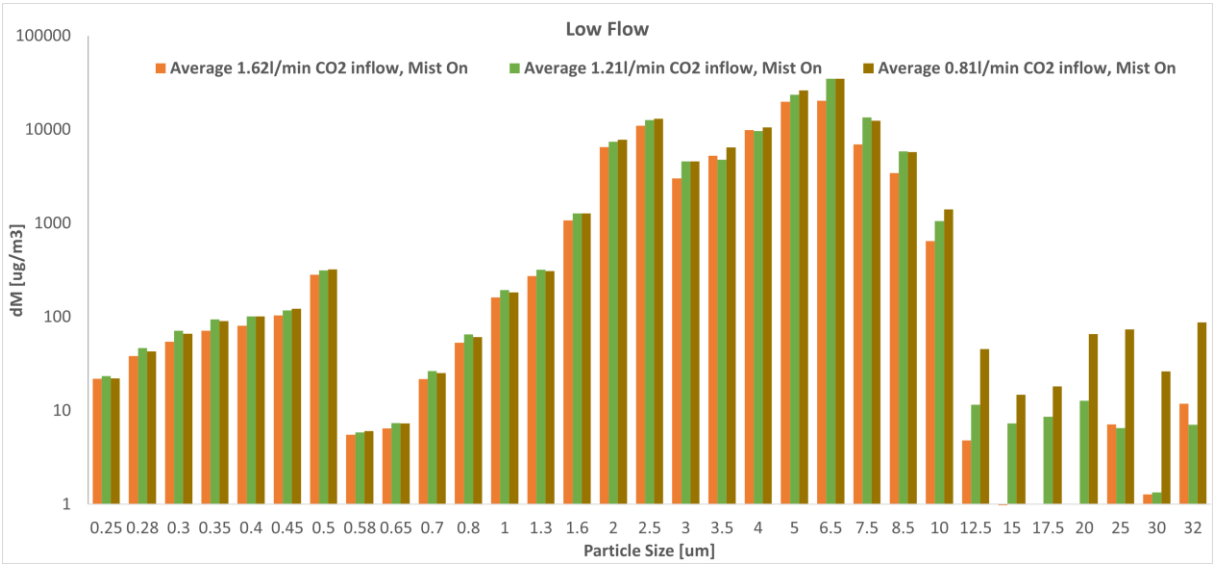

Figure 18 Particle distribution by mass of water aerosol and air infused CO_2. The air flow is low. Measurement was done before separation.

The particle size distribution for mist generation with NaOH of 3 different concentrations can be seen in Figure 19. The distribution shown in this figure is very similar to that of mist in previous figures, different bulk flow speed. A trend in how the differences in the size

distribution varies depending on NaOH concentration cannot be seen. The distribution is similar along most of the particle sizes, the biggest percentual deviations can be seen in the size range of 17.5-32µm. However, these deviations are for masses that are several orders of magnitude less than the range of 1-10µm. Any uncertainties can be said to be the same of what was observed discussed earlier for mist generated by only water.

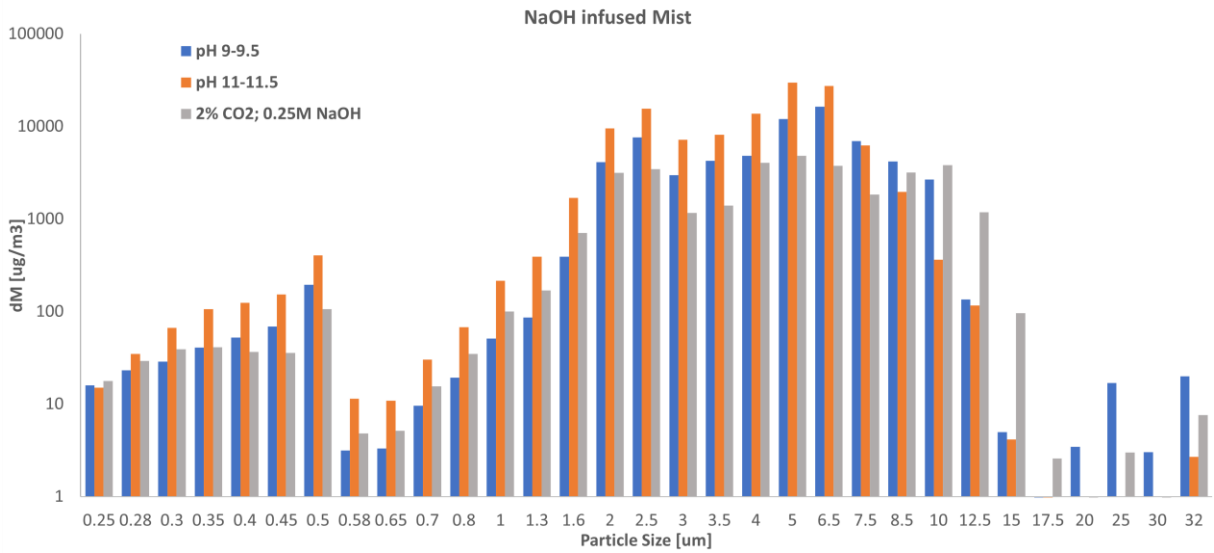

Figure 19 Particle distribution by mass of three different concentrations of NaOH aerosol, and air infused CO_2. The air flow is low. Measurement was done before separation.

5 CONCLUSION

To summarize the experimental procedure and results, it can be said that while the experimental setup itself proved to be very flexible it still had several limitations. It was possible to measure particle size distribution and CO_2 concentration simultaneously, however, it was only possible for when particle size was measured before the separating process at bulk flow of 5m/s at most. There was not enough space for more simultaneous measurements after the separating process. Due to this, size can be said to be its main limitation. However, the operation of the setup was successful without any issues arising. Issues while in operation were kept external, such as the measuring equipment.

Additionally, the measuring equipment available made it difficult to track the CO_2 concentration, due to the low concentration used, as well as the CO_2 inflow being unstable due to such low flows. For future considerations, measuring instruments capable of measuring higher CO_2 concentrations should be made of use. This would make any smaller changes be more easily tracked, in comparison to that of smaller changes in a smaller range. Furthermore, measurements in several more points in the experimental system should be taken into account, specifically for the particle size measurements, as they were only measured before the separation, this would also need for there to be adjustments in the setup regarding its size, due to the relatively small path in comparison to the potential residence time of CO_2 to diffuse into or react with the absorbent.

A suggestion for how to scale up the system is by lengthen the pipe sections, specifically the pipe sections directly before and after the separator. This would ensure a longer time for the absorption process to occur, as well as for the flow after the separator to stabilize, in addition to making it possible for simultaneous measurement of particle size and CO_2 concentration after the separation process.

6 NOMENCLATURE

6.1 ROMAN SYMBOLS

Table 1 List of all used Roman symbols, with accompanying description and units.

Symbol	Meaning	Unit
A	Area	[m^2]
c	Concentration	[-]
C	Concentration	[-]
d	Particle diameter	[m]
D	Droplet mean diameter	[m]
F	Frequency	[s^{-1}]
g	Gravitation acceleration	[m/s^2]
H	Henry's lawn constant	[M/Pa]
k	Dimensionless parameter	[-]
n	Dimensionless parameter	[-]
p	Partial pressure	[Pa]
Q	Volumetric flow	[m^3/s]
q	Volumetric flow	[m^3/s]
R	Disc stack radius	[m]
T	Temperature	[K]
U	Velocity	[m/s]
v	Particle velocity	[m/s]

6.2 GREEK SYMBOLS

Table 2 List of all Greek symbols used, with accompanying description and units.

Symbol	Meaning	Unit
ρ	Density	[kg/m^3]
μ	Dynamic Viscosity	[kg/s*m]
η	Grade efficiency	[-]
λ	Wavelength	[m]
ω	Angle velocity	[rad/s]
φ	Disc stack angle	[rad]

6.3 SUBSCRIPT

Table 3 List of all used subscripts, with accompanying description.

Symbol	Meaning
100	100%
air	Property of air
c	Critical
CO_2	Property of air CO_2
cp	Denotes form of Henry's constant
e	Settling
g	In the gravitational direction
gs	Gas and liquid-gas interface
i	Inner
ls	Liquid and liquid-gas interface
o	Outer
s	Used for constants at 298.15K

7 REFERENCES

[1]A. Cambiella, J. M. Benito, C. Pazos, and J. Coca, “Centrifugal separation efficiency in the treatment of waste emulsified oils,” Chemical Engineering Research and Design, vol. 84, no. 1, pp. 69–76, 2006.

[2]A. D. DUKES III, “Measuring the Henry’s law constant for carbon dioxide and water with UV-visible absorption spectroscopy,” Analytical Sciences, vol. 36, no. 8, pp. 971–975, 2020.

[3]A. Dalmoro, A. A. Barba, and M. d’Amore, “Analysis of size correlations for microdroplets produced by ultrasonic atomization,” The Scientific World Journal, vol. 2013, pp. 1–7, 2013.

[4] A. I. Clarkson, M. Bulmer, and N. J. Titchener-Hooker, “Pilot-scale verification of a computer-based simulation for the centrifugal recovery of biological particles,” Bioprocess Engineering, vol. 14, no. 2, pp. 81–89, 1996.

[5]A. Penttilä, C. Dell’Era, P. Uusi-Kyyny, and V. Alopaeus, “The Henry's law constant of n2o and CO2 in aqueous binary and ternary amine solutions (MEA, DEA, Dipa, MDEA, and Amp),” Fluid Phase Equilibria, vol. 311, pp. 59–66, 2011.

[6]A. Sood and S. Vyas, “Carbon capture and sequestration- A Review,” IOP Conference Series: Earth and Environmental Science, vol. 83, p. 012024, 2017.

[7]B. Avvaru, M. N. Patil, P. R. Gogate, and A. B. Pandit, “Ultrasonic atomization: Effect of liquid phase properties,” Ultrasonics, vol. 44, no. 2, pp. 146–158, 2006.

[8]B. Xue, Y. Yu, J. Chen, X. Luo, and M. Wang, “A comparative study of MEA and DEA for post-combustion CO2 Capture with different process configurations,” International Journal of Coal Science & Technology, vol. 4, no. 1, pp. 15–24, 2016.

[9]B.-S. Park and S.-M. Kang, “Spatial distribution of negative air ions produced by an ultrasonic mist maker,” Journal of the Korean Physical Society, vol. 58, no. 6, pp. 1618–1621, 2011.

[10]C. Ambler, “Theory of centrifugation,” Industrial & Engineering Chemistry, vol. 53, no. 6, pp. 430–433, 1961.

[11]C. Halliday and T. A. Hatton, “Sorbents for the capture of CO2 and other acid gases: A Review,” Industrial & Engineering Chemistry Research, vol. 60, no. 26, pp. 9313–9346, 2021.

[12]C. Inge, P. Franzén, C. Erdmann, and F. Zitarosa, “Disc type centrifuges for cleaning blow-by gas at PC engines,” MTZ worldwide, vol. 78, no. 9, pp. 54–59, 2017.

[13]C. Rodes, T. Smith, R. Crouse, and G. Ramachandran, “Measurements of the size distribution of aerosols produced by Ultrasonic humidification,” Aerosol Science and Technology, vol. 13, no. 2, pp. 220–229, 1990.

[14]C.-C. Lin, W.-T. Liu, and C.-S. Tan, “Removal of carbon dioxide by absorption in a rotating packed bed,” Industrial & Engineering Chemistry Research, vol. 42, no. 11, pp. 2381–2386, 2003.

[15]D. Im, K. Roh, J. Kim, Y. Eom, and J. H. Lee, “Economic assessment and optimization of the SELEXOL process with novel additives,” International Journal of Greenhouse Gas Control, vol. 42, pp. 109–116, 2015.

[16]F. Lucile, P. Cézac, F. Contamine, J.-P. Serin, D. Houssin, and P. Arpentinier, “Solubility of carbon dioxide in water and aqueous solution containing sodium hydroxide at temperatures from (293.15 to 393.15) K and pressure up to 5 MPA: Experimental measurements,” Journal of Chemical & Engineering Data, vol. 57, no. 3, pp. 784–789, 2012.

[17]F. Yi, H.-K. Zou, G.-W. Chu, L. Shao, and J.-F. Chen, “Modeling and experimental studies on absorption of CO2 by Benfield Solution in rotating packed bed,” Chemical Engineering Journal, vol. 145, no. 3, pp. 377–384, 2009.

[18]F. Zeman, “Energy and material balance of CO2 Capture from ambient air,” Environmental Science & Technology, vol. 41, no. 21, pp. 7558–7563, 2007.

[19]H. Hikita, S. Asai, and T. Takatsuka, “Absorption of carbon dioxide into aqueous sodium hydroxide and sodium carbonate-bicarbonate solutions,” The Chemical Engineering Journal, vol. 11, no. 2, pp. 131–141, 1976.

[20]H. Kobara, M. Tamiya, A. Wakisaka, T. Fukazu, and K. Matsuura, “Relationship between the size of mist droplets and ethanol condensation efficiency at ultrasonic atomization on ethanol-water mixtures,” AIChE Journal, 2009.

[21]H. Lu, H. Wang, Y. Liu, M. Wang, J. Hu, and Q. Yang, “Substance transfer behavior controlled by droplet internal circulation,” Chemical Engineering Journal, vol. 393, p. 124657, 2020.

[22]H. W. Pennline, D. R. Luebke, K. L. Jones, C. R. Myers, B. I. Morsi, Y. J. Heintz, and J. B. Ilconich, “Progress in carbon dioxide capture and separation research for gasification-based Power Generation Point Sources,” Fuel Processing Technology, vol. 89, no. 9, pp. 897–907, 2008.

[23]H.-T. Wu and C.-C. Chung, “Effects of vapor pressure of desiccant solution on mass transfer performance for a spray-bed absorber,” Processes, vol. 9, no. 9, p. 1517, 2021.

[24]IEA, CO2 Emissions from Fuel Combustion 2019, OECD, 2019.

[25]IPCC, “Press release,” IPCC Intergovernmental Panel on Climate Change. [Online]. Available: https://www.ipcc.ch/report/ar6/wg3/resources/press/press-release. [Accessed: 30-May-2022].

[26]J. K. Stolaroff, D. W. Keith, and G. V. Lowry, “Carbon dioxide capture from atmospheric air using sodium hydroxide spray,” Environmental Science & Technology, vol. 42, no. 8, pp. 2728–2735, 2008.

[27]J. P. Maybury, K. Mannweiler, N. J. Titchener-Hooker, M. Hoare, and P. Dunnill, “The performance of a scaled down industrial disc stack centrifuge with a reduced feed material requirement,” Bioprocess Engineering, vol. 18, no. 3, p. 191, 1998.

[28]J. Porstendörfer, J. Gebhart, and G. Röbig, “Effect of evaporation on the size distribution of nebulized aerosols,” Journal of Aerosol Science, vol. 8, no. 6, pp. 371–380, 1977.

[29]J. V. Nascimento, T. M. Ravagnani, and J. A. Pereira, “Experimental study of a rotating packed bed distillation column,” Brazilian Journal of Chemical Engineering, vol. 26, no. 1, pp. 219–226, 2009.

[30]J.-G. Shim, D. W. Lee, J. H. Lee, and N.-S. Kwak, “Experimental study on capture of carbon dioxide and production of sodium bicarbonate from sodium hydroxide,” Environmental Engineering Research, vol. 21, no. 3, pp. 297–303, 2016.

[31]K. A. Mumford, Y. Wu, K. H. Smith, and G. W. Stevens, “Review of solvent based carbon-dioxide capture technologies,” Frontiers of Chemical Science and Engineering, vol. 9, no. 2, pp. 125–141, 2015.

[32]K. Mannweiler and M. Hoare, “The scale-down of an industrial disc stack centrifuge,” Bioprocess Engineering, vol. 8, no. 1-2, pp. 19–25, 1992.

[33]M. Ajay and T. N. C. Anand, "STUDY OF ULTRASONIC ATOMIZATION," 2013.

[34]M. Yoo, S.-J. Han, and J.-H. Wee, “Carbon dioxide capture capacity of sodium hydroxide aqueous solution,” Journal of Environmental Management, vol. 114, pp. 512–519, 2013.

[35]O. Ramalho, G. Wyart, C. Mandin, P. Blondeau, P.-A. Cabanes, N. Leclerc, J.-U. Mullot, G. Boulanger, and M. Redaelli, “Association of Carbon Dioxide with indoor air pollutants and exceedance of health guideline values,” Building and Environment, vol. 93, pp. 115–124, 2015.

[36]P. Deepu, C. Peng, and S. Moghaddam, “Dynamics of ultrasonic atomization of droplets,” Experimental Thermal and Fluid Science, vol. 92, pp. 243–247, 2018.

[37]Q.-J. Yang, Q. Mao, and W. Cao, “Numerical simulation of the Marangoni Flow on mass transfer from single droplet with different Reynolds numbers,” Colloids and Surfaces A: Physicochemical and Engineering Aspects, vol. 639, p. 128385, 2022.

[38]R. Battisti, R. A. F. Machado, and C. Marangoni, “A background review on falling film distillation in wetted-wall columns: From fundamentals towards Intensified Technologies,” Chemical Engineering and Processing - Process Intensification, vol. 150, p. 107873, 2020.

[39]R. J. Lang, “Ultrasonic atomization of liquids,” The Journal of the Acoustical Society of America, vol. 34, no. 1, pp. 6–8, 1962.

[40]R. Rajan and A. B. Pandit, “Correlations to predict droplet size in ultrasonic atomisation,” Ultrasonics, vol. 39, no. 4, pp. 235–255, 2001.

[41]R. Sander, “Compilation of Henry's Law Constants (version 4.0) for water as solvent,” Atmospheric Chemistry and Physics, vol. 15, no. 8, pp. 4399–4981, 2015.

[42]T. Kudo, K. Sekiguchi, K. Sankoda, N. Namiki, and S. Nii, “Effect of ultrasonic frequency on size distributions of nanosized mist generated by ultrasonic atomization,” Ultrasonics Sonochemistry, vol. 37, pp. 16–22, 2017.

[43]T. N.Borhani and M. Wang, “Role of solvents in CO2 Capture Processes: The Review of selection and design methods,” Renewable and Sustainable Energy Reviews, vol. 114, p. 109299, 2019.

[44]W. H. Tay, K. K. Lau, and A. M. Shariff, “High frequency ultrasonic-assisted CO2 absorption in a high pressure water batch system,” Ultrasonics Sonochemistry, vol. 33, pp. 190–196, 2016.

[45]W.-H. Chen, “Microphysics of atmospheric carbon dioxide uptake by a cloud droplet containing a solid nucleus,” Journal of Geophysical Research, vol. 108, no. D15, 2003.

[46]W.-H. Chen, S.-M. Chen, and C.-I. Hung, “Carbon dioxide capture by single droplet using selexol, Rectisol and water as absorbents: A theoretical approach,” Applied Energy, vol. 111, pp. 731–741, 2013.

[47]W.-H. Chen, “Unsteady absorption of sulfur dioxide by an atmospheric water droplet with internal circulation,” Atmospheric Environment, vol. 35, no. 13, pp. 2375–2393, 2001.

[48]Z. Xu, K. Yasuda, and X. Liu, “Simulation of the formation and characteristics of Ultrasonic Fountain,” Ultrasonics Sonochemistry, vol. 32, pp. 241–246, 2016.

8 APPENDIX

Figure 20 The whole experimental setup.

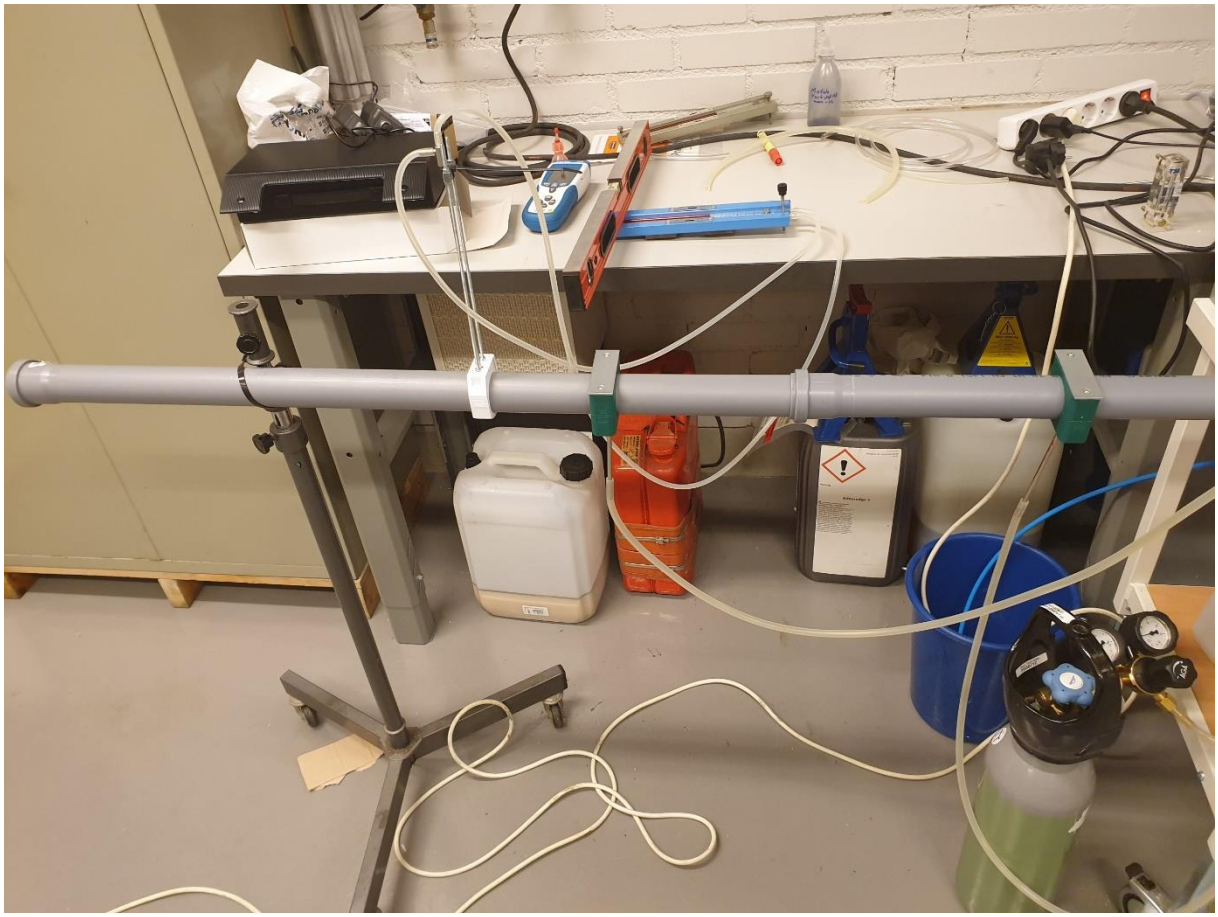

Figure 21 Initial piping section of the experimental setup.

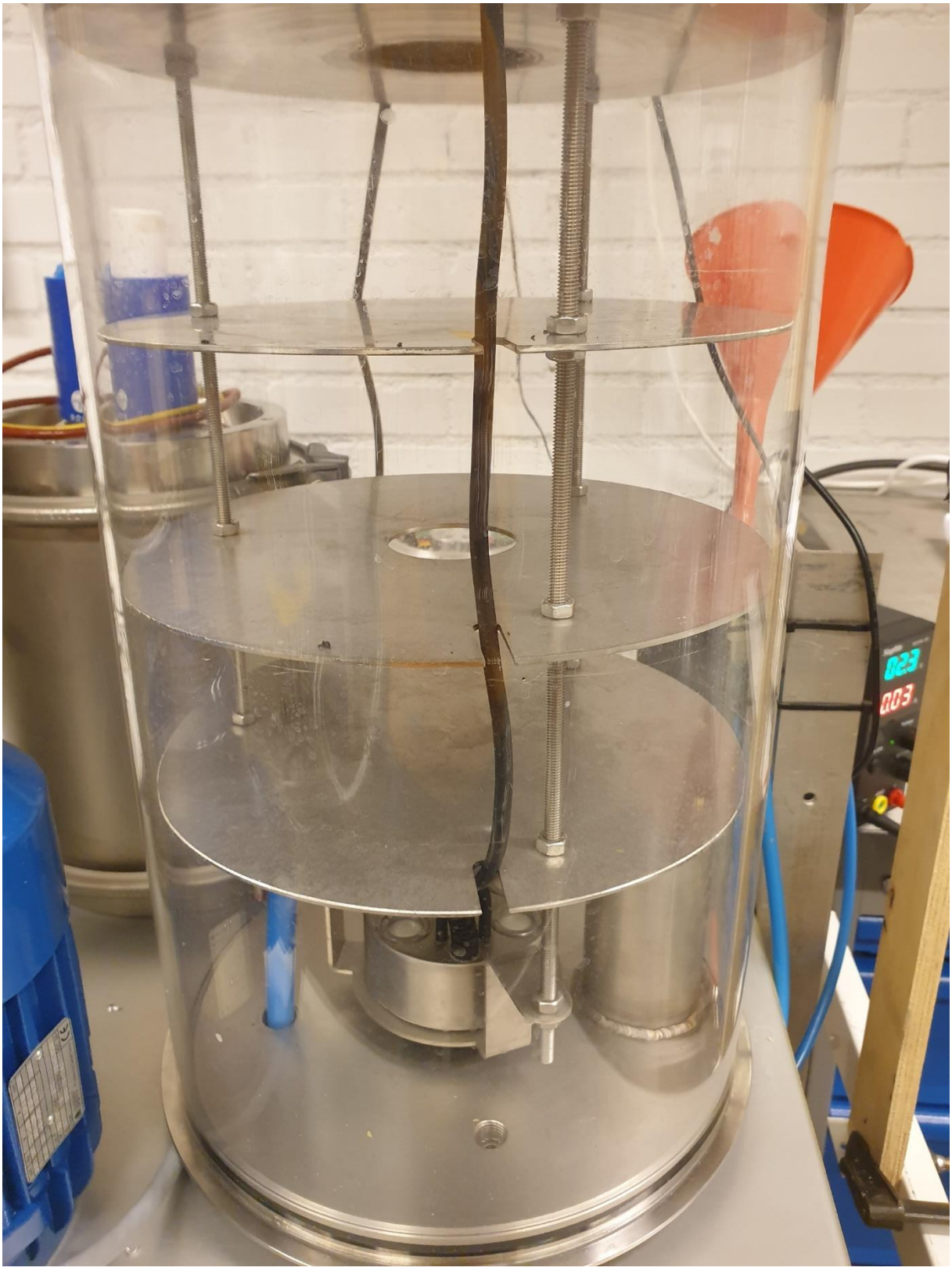

Figure 22 Mist chamber section of the experimental setup.

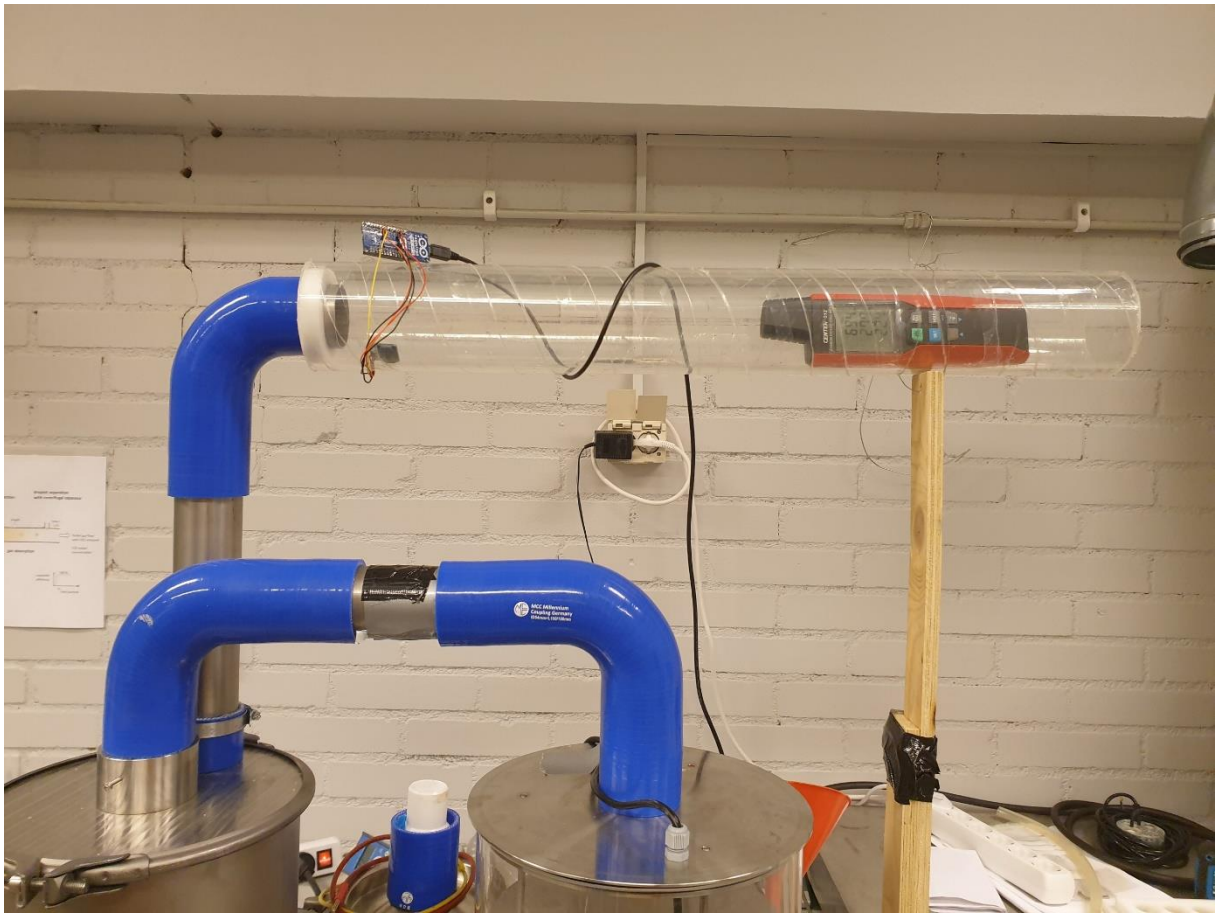

Figure 23 Transition piping section between mist chamber and the centrifuge; as well as the outlet.